



Graziosi, F., Arduini, J., Furlani, F., Giostra, U., Cristofanelli, P., Fang, X., ...
Maione, M. (2017). European emissions of the powerful greenhouse gases
hydrofluorocarbons inferred from atmospheric measurements and their
comparison with annual national reports to UNFCCC. *Atmospheric
Environment*, 158. <https://doi.org/10.1016/j.atmosenv.2017.03.029>

Peer reviewed version

License (if available):
CC BY-NC-ND

Link to published version (if available):
[10.1016/j.atmosenv.2017.03.029](https://doi.org/10.1016/j.atmosenv.2017.03.029)

[Link to publication record in Explore Bristol Research](#)
PDF-document

This is the final published version of the article (version of record). It first appeared online via Elsevier at <https://doi.org/10.1016/j.atmosenv.2017.03.029> . Please refer to any applicable terms of use of the publisher.

University of Bristol - Explore Bristol Research

General rights

This document is made available in accordance with publisher policies. Please cite only the published version using the reference above. Full terms of use are available:
<http://www.bristol.ac.uk/pure/about/ebr-terms>

1 **European emissions of the powerful greenhouse gases hydrofluorocarbons inferred from**
2 **atmospheric measurements and their comparison with annual national reports to UNFCCC.**

3

4 F. Graziosi^{1,2}, J. Arduini^{1,3}, F. Furlani^{1,2}, U. Giostra^{1,2}, P. Cristofanelli³, X. Fang⁴, O. Hermanssen⁵,
5 C. Lunder⁵, G. Maenhout⁶, S. O'Doherty⁷, S. Reimann⁸, N. Schmidbauer⁵, M.K. Vollmer⁸, D.
6 Young⁷ and M. Maione^{1,2,3}

7

8 ¹ Department of Pure and Applied Sciences, University of Urbino, Urbino, Italy

9 ² CINFAI (National Inter-University Consortium for Physics of the Atmosphere and Hydrosphere),
10 Rome, Italy

11 ³ Institute of Atmospheric Sciences and Climate, National Research Council, Bologna, Italy

12 ⁴ Centre for Global Change Science, Massachusetts Institute of Technology, Cambridge,
13 Massachusetts, USA

14 ⁵ Norwegian Institute for Air Research, Kjeller, Norway

15 ⁶ Joint Research Centre of the European Commission, Ispra (VA), Italy

16 ⁷ Atmospheric Chemistry Research Group, School of Chemistry, University of Bristol, Bristol, UK

17 ⁸ Laboratory for Air Pollution and Environmental Technology, Empa, Swiss Federal Laboratories
18 for Materials Science and Technology, Dübendorf, Switzerland

19

20 Corresponding author: michela.maione@uniurb.it

21

22 **Abstract**

23 Hydrofluorocarbons are powerful greenhouse gases developed by industry after the phase-out of the
24 ozone depleting chlorofluorocarbons and hydrochlorofluorocarbons required by the Montreal
25 Protocol. The climate benefit of reducing the emissions of hydrofluorocarbons has been widely
26 recognised, leading to an amendment of the Montreal Protocol (Kigali Amendment) calling for
27 developed countries to start to phase-down hydrofluorocarbons by 2019 and in developing countries
28 to follow with a freeze between 2024 and 2028. In this way, nearly half a degree Celsius of
29 warming would be avoided by the end of the century. Hydrofluorocarbons are also included in the
30 basket of gases controlled under the Kyoto Protocol of the United Nations Framework Convention
31 on Climate Change. Annex I parties to the Convention submit annual national greenhouse gas

32 inventories based on a bottom-up approach, which relies on declared anthropogenic activities. Top-
33 down methodologies, based on atmospheric measurements and modelling, can be used in support to
34 the inventory compilation. In this study we used atmospheric data from four European sites
35 combined with the FLEXPART dispersion model and a Bayesian inversion method, in order to
36 derive emissions of nine individual hydrofluorocarbons from the whole European Geographic
37 Domain and from twelve regions within it, then comparing our results with the annual emissions
38 that the European countries submit every year to the United Nations Framework Convention on
39 Climate Change, as well as with the bottom-up Emissions Database for Global Atmospheric
40 Research. We found several discrepancies when considering the specific compounds and on the
41 country level. However, an overall agreement is found when comparing European aggregated data,
42 which between 2008 and 2014 are on average 84.2 ± 28.0 Tg-CO₂-eq·yr⁻¹ against the 95.1 Tg-CO₂-
43 eq·yr⁻¹ reported by UNFCCC in the same period. Therefore, in agreement with other studies, the
44 gap on the global level between bottom-up estimates of Annex I countries and total global top-down
45 emissions should be essentially due to emissions from non-reporting countries (non-Annex I).

46

47 **1.Introduction**

48 The increase of hydrofluorocarbon (HFC) concentrations in the atmosphere has been recognised as
49 a major driver for climate change (IPCC, 1990; 2013). HFCs have been produced by industry for a
50 variety of uses (refrigerants, foam blowing agents, propellants, solvents, fire retardants, besides the
51 non-reported military uses) as a replacement of the ozone-depleting chlorofluorocarbons (CFCs)
52 and hydrochlorofluorocarbons (HCFCs), whose emissive uses were phased-out under the Montreal
53 Protocol (MP) on Substances that Deplete the Ozone Layer (UNEP, 1987). The MP, through the
54 phase-out of production and consumption of ozone depleting substances, led to a significant decline
55 in CFC and HCFC atmospheric concentrations. Originally HFCs, having only an indirect impact on
56 the ozone layer (Hurwitz et al., 2015), were not under the MP regulatory framework. Yet the
57 potential climate benefits of reducing HFC emissions has been recognised by the UNEP-CCAC
58 (Climate and Clean Air Coalition), an international initiative aiming at catalysing rapid reductions
59 in short-lived climate pollutants (SLCPs), based on the assumption that a timely reduction of
60 SLCPs can slow the rate of climate change within the first half of this century, i.e. before the long
61 lived CO₂ reduction measures will take effect (Velders et al., 2009; UNEP, 2011; Shindell et al.,
62 2012; Xu et al., 2013). In addition, it has been estimated that, due to the high GWPs of the HFCs,
63 without direct regulation the HFC atmospheric increase could lead to 14 to 27% of the increase in
64 CO₂ radiative forcing (RF) under the range of IPCC (Intergovernmental Panel on Climate Change)

65 business-as usual scenarios from 2010 to 2050 (Velders et al., 2012 and 2015; Montzka and
66 Reimann, 2011).

67 Consequently, in 2015 several formal proposals were issued (UNEP 2015a, b, c, d) to amend the
68 Montreal Protocol to phase down the production and consumption of HFCs. This resulted in the
69 Kigali Amendment to the MP agreed during the 28th meeting of the parties (MOP28) in October
70 2016, calling for developed countries to start to phase-down HFCs by 2019 and in developing
71 countries to follow with a freeze of HFC consumption levels between 2024 and 2028
72 (www.unep.org). This legally binding agreement would avoid nearly half a degree Celsius of
73 warming by the end of the century.

74 In addition, HFCs were regulated under the United Nations Framework Convention on Climate
75 Change (UNFCCC) Kyoto Protocol and their production and use were subject only to voluntary
76 regulation (UNFCCC, 1997). Parties included in Annex I to the UNFCCC (Annex I Parties) have
77 been required to submit annual national GHG inventories, covering emissions and removals of the
78 six direct GHGs included in the so-called Kyoto basket: carbon dioxide (CO₂), methane (CH₄),
79 nitrous oxide (N₂O), the F-gases (hydrofluorocarbons, HFCs and perfluorocarbons, PFCs) and
80 sulfur hexafluoride (SF₆). Each gas is weighted by its 100-year global warming potential (GWP)
81 and aggregated to give total GHG emissions in CO₂ equivalents (UNFCCC, 2006). The reliability
82 of the emission data reported by the parties to UNFCCC is crucial in assessing the Parties
83 compliance with the Kyoto Protocol and therefore in determining the Protocol's effectiveness.
84 Following the IPCC guidelines (IPCC, 2006), the UNFCCC requires only bottom-up reporting,
85 which relies on declared anthropogenic activities, that for F-gases are industrial processes and
86 product use, and on emission factors for the release into the atmosphere. However, the combination
87 of atmospheric measurements of GHGs and atmospheric modelling, the so-called 'top-down
88 approach', can be efficiently used for estimating emissions from the global to the country level (e.g.
89 Bergamaschi et al., 2004; Nisbet and Weiss, 2010; Manning et al., 2011; Weiss and Prinn, 2011;
90 Graziosi et al., 2015; Henne et al., 2016).

91 Among the Kyoto gases HFCs are considered particularly suitable for estimating emissions using
92 inverse modelling as they are solely of anthropogenic origin and sufficiently long-lived. This
93 approach could be used in support of the quality assurance of the inventories, whose uncertainty is
94 only loosely constrained among different countries (IPCC, 2006). In the past decade, the increased
95 capability of producing high-quality atmospheric data of HFCs in combination with rapidly
96 developing inverse modelling techniques has allowed the realisation of a number of studies
97 reporting top-down HFC emission estimates from the global to the regional scale (Yokouchi et al.,

98 2006; Grealley et al., 2007; Stemmler et al., 2007; Stohl et al., 2009; Miller et al., 2010; Montzka et
99 al., 2010; Li et al., 2010; Stohl et al., 2010; Vollmer et al., 2011; Brunner et al., 2012; Keller et al.,
100 2012; Yao et al., 2012; O’ Doherty et al. 2014; Rigby et al., 2014; Fang et al., 2016; Hu et al.,
101 2015; Lunt et al., 2015; Simmonds et al., 2016). The inversion results have shown different degrees
102 of disagreement with HFC bottom-up emissions as reported to the UNFCCC, especially when the
103 individual species are considered rather than the aggregated numbers (Lunt et al., 2015). In
104 addition, for those HFCs whose commercial production has started only in recent years and whose
105 annual reports are lacking or whose obligations for publicly reporting of data are lifted because of
106 industrial confidentiality, the use of the top-down approach can serve to monitor the emission trends
107 and to raise early warning in case of inconsistencies or incompleteness.

108 Since emissions control legislation is based on national or regional numbers, it would be important
109 to assess the annual reports through the use of top-down methods at these same geographic scales.
110 In Europe the reference regulations on fluorinated greenhouse gases are the EU mobile air
111 conditioning (MAC) directive (EU, 2006), which bans the use of HFC-134a in motor vehicle AC
112 from 2017, and the revised F-gas regulation (EU, 2014) which bans the use of high-GWP HFCs in
113 other sectors starting in 2015 and also contains a phase down of HFC consumption from a base
114 level. This Regulation also states “Effective monitoring of fluorinated greenhouse gas emissions is
115 critical for tracking progress towards the achievement of emission reduction targets and for
116 assessing the impact of this Regulation”.

117 Using atmospheric data from four European sites combined with the Lagrangian 3-D particle
118 dispersion model FLEXPART and a Bayesian inversion method, we estimated the emissions of
119 nine individual HFCs from the whole European Geographic Domain (EGD) and from twelve
120 regions (representing individual countries or group of countries) within the EGD. These numbers
121 were then compared with the annual emissions that the European countries submit to the UNFCCC.
122 The observed discrepancies are then discussed. The list of the HFCs considered in this study is
123 reported in Table 1, where their main characteristics in relation to their impact on climate (i.e.
124 Radiative Efficiency and GWP) are given. The study period is from January 2003 to December
125 2014, although for some compounds shorter time series are available. In addition, we compared our
126 results with the bottom-up Emissions Database for Global Atmospheric Research
127 (EDGARv4.2FT2010, hereinafter EDGAR), a database that estimates global emission inventories
128 of anthropogenic GHGs on a country, region and grid basis up to 2010.

129

130 Table 1: List of the compounds considered in this study. Lifetime, radiative efficiency and GWP values are
 131 from Myhre et al. (2013) for all the compounds, excluding HFC-365mfc for which values are as in UNEP-
 132 TEAP (2010).

133

Industrial Name	Chemical formula	Lifetime (Years)	Radiative Efficiency ($\text{W m}^{-2} \text{ppb}^{-1}$)	GWP 20 Years	GWP 100 Years	Main use
HFC-32	CH_2F_2	5.2	0.11	2430	677	Refrigerant
HFC-125	CHF_2CF_3	28.2	0.23	6090	3170	Refrigerant
HFC-134a	CH_2FCF_3	13.4	0.19	3710	1300	Refrigerant
HFC-143a	CH_3CF_3	47.1	0.16	6940	4800	Refrigerant
HFC-152a	CH_3CHF_2	1.5	0.10	506	138	Foam blowing
HFC-227ea	$\text{CF}_3\text{CHFCF}_3$	38.9	0.26	5360	3350	Fire retardant
HFC-236fa	$\text{CF}_3\text{CH}_2\text{CF}_3$	242	0.24	6940	8060	Fire retardant, Refrigerant
HFC-245fa	$\text{CHF}_2\text{CH}_2\text{CF}_3$	7.7	0.24	2920	858	Foam blowing
HFC-365mfc	$\text{CH}_3\text{CF}_2\text{CH}_2\text{CF}_3$	8.6	0.22	2660	804	Foam blowing

134

135 2. Method

136 2.1 Observations

137 In Europe, atmospheric measurement data for a wide range of HFCs are available at four sites:
 138 Jungfraujoch (JFJ), Switzerland (CH), Mace Head (MHD), Ireland (IE), Monte Cimone (CMN),
 139 Italy (IT), and Zeppelin (ZEP), Norway, Spitzbergen (NO). Through the use of gas
 140 chromatographic-mass spectrometric instrumentation (Miller et al., 2008; Maione et al., 2013),
 141 these stations are providing long-term, high-frequency and high-precision measurements of several
 142 halogenated gases. This is the result of a coordination effort that started in 2001 under the European
 143 SOGE (System for Observations of Halogenated Greenhouse Gases in Europe) Project. The four
 144 European stations are embedded in the AGAGE (Advanced Global Atmospheric Gases Experiment)
 145 programme (Prinn et al., 2000), which, together with the NOAA/GMD (National Oceanic and

146 Atmospheric Administration/Global Monitoring Division) (Montzka et al., 1994) and the NIES
147 (National Institute for Environmental Studies, Japan) (Yokouchi et al., 2006) monitoring networks,
148 represents the most important observation system for a wide range of ozone depleting and climate
149 altering species. Details of the monitoring network and on the analytical methods are given in the
150 Supplementary Material (SM) section.

151 2.2 Inverse Modelling

152 The approach that we used for this study combines the high-frequency trace gas observations with
153 an atmospheric particle dispersion model and a Bayesian inversion. To simulate transport to the
154 receptor sites, we used trajectories obtained with the 3-D FLEXPART v-9.02 dispersion model
155 (Stohl et al., 1998; 2005; Seibert and Frank, 2004) run every three hours for 20 days backward,
156 driven by operational three-hourly meteorological data at 1°x 1° resolution from the European
157 Centre for Medium-Range Weather Forecasts (ECMWF). This allowed us to obtain the sensitivity
158 of the receptor to the source, also defined as the source receptor relationship (SRR) which in a
159 particular grid cell is proportional to the particle residence time in that cell and measures the
160 simulated mixing ratio that a source of unit strength (1 kg s^{-1}) in the cell would produce at the
161 receptor (Stohl et al., 2009). Multiplying the SRR by the emission flux taken from an appropriate
162 emission inventory (the *a priori* emission field), the simulated mixing ratio at the receptor to be
163 compared with the observations is obtained. After having tested two different *a priori* emission
164 fields (see paragraph 3 in the SM), we selected as *a priori* the UNFCCC inventory that gives the
165 best correlation coefficient between the simulated times series and the observations. Finally, the *a*
166 *posteriori* emission field was obtained through the Bayesian inversion method developed by Seibert
167 (2000; 2001), improved by Eckhardt et al. (2008) and Stohl et al. (2009; 2010) and recently applied
168 by Maione et al. (2014) and Graziosi et al. (2015). The uncertainty associated with the obtained
169 EGD emission values resulted to be 35%, averaged over time and compound. Details of the inverse
170 modelling method are given in the SM (paragraph 3).

171

172

173 **3. Results and Discussion**

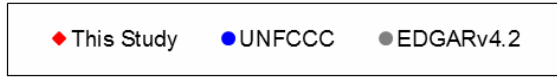
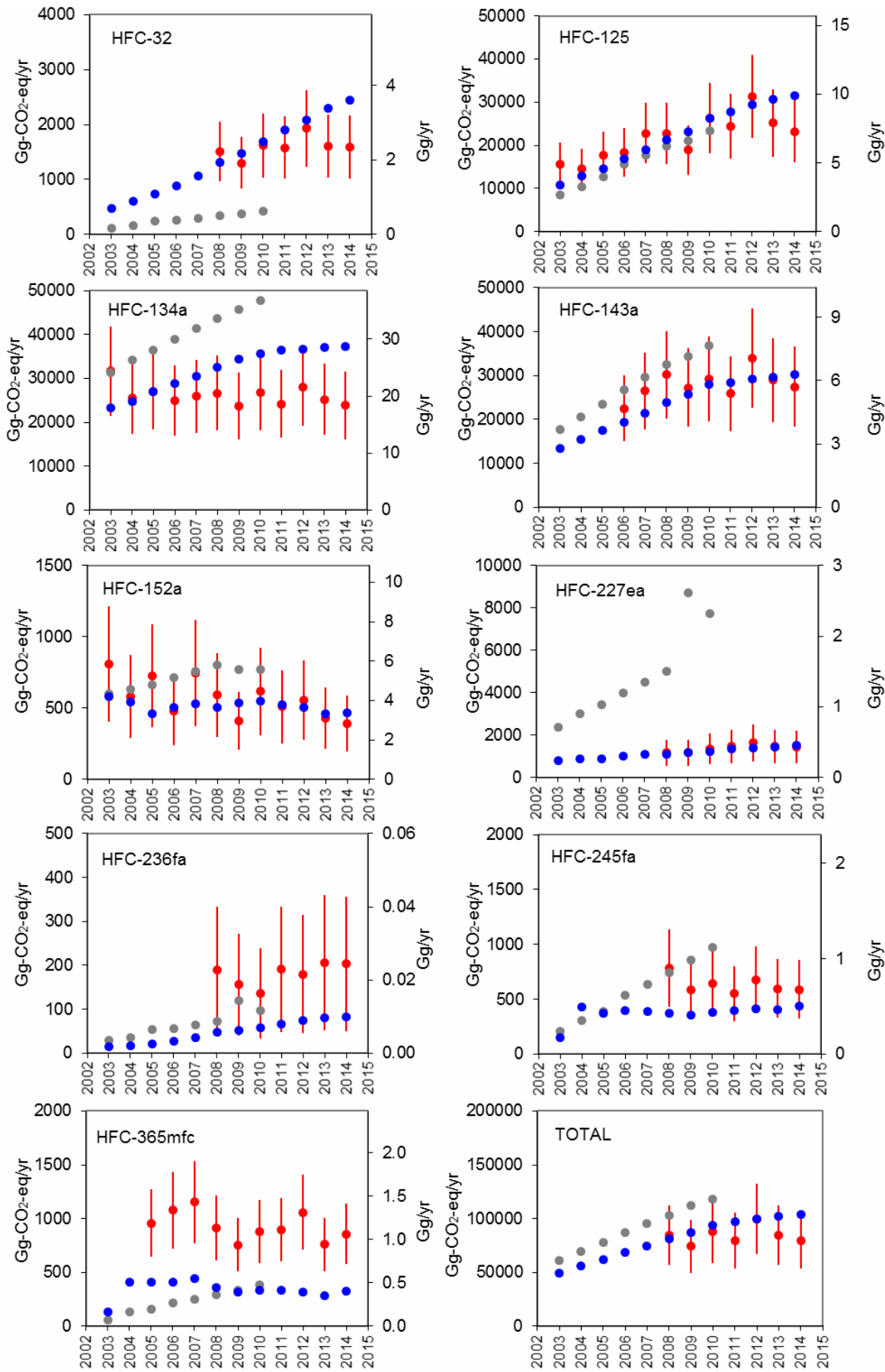
174

175 3.1 European emissions

176

177 In Figure 1 EGD yearly emissions estimated through the proposed method are reported for nine
178 HFCs (red dots). The uncertainty in the estimates is derived from the model (see SM, paragraph 3).

179 Since not all stations started to monitor the HFCs considered in this study at the same time, the
180 inversions have been performed for those years in which data from at least two stations were
181 available. Detailed annual emissions for each compound and the associated percent error from the
182 EGD and from the twelve macro-areas considered in this study are reported in Table 2S in the SM.
183 UNFCCC estimates up to 2014 (blue dots) are reported for each compound and the comparison
184 with the inversion results is discussed. For the sake of completeness EDGAR estimates up to 2010
185 (grey dots) are also given. In many instances large differences between the two bottom-up data sets
186 are observed. Such differences in the annual emissions can be due to inconsistencies in the base
187 year estimates for each country, which in EDGAR are based on AFEAS (Alternative Fluorocarbons
188 Environmental Acceptability Study) data. Differences in emission trends can be due to the use of
189 different proxies, like e.g. the use of a relatively strong growth curve (often linearly increasing from
190 1990 onwards), as in the case of the use of air conditioning in European cars, or of fire retardants.
191 In the following we provide, for each compound, details on emission fluxes and their temporal
192 trends. It should be noted that we found that only three out of nine HFCs (namely, HFC-125, 152a
193 and 227ea) exhibit a significant (significance level $\alpha = 0.01$) linear trend. UNFCCC emission data
194 exhibit, during the period in common with the inversion, a significant ($\alpha = 0.01$) linear trend for all
195 the compounds considered, with the exception of HFC-152a. We did not evaluate trends of EDGAR
196 emissions, since the overlapping with our estimates is for the majority of the compounds limited to
197 three years.



199 Figure 1. Emissions of nine HFCs from the European Geographic Domain from January 2003 to December 2014.
200 Emissions are given in Gg yr⁻¹ (right axis) and in Gg-CO₂-eq yr⁻¹ (left axis). TOTAL = aggregated emissions of nine
201 HFCs. Red: this study; Blue: UNFCCC; Grey: EDGARv4.2FT2010.
202

203 *HFC-32*

204 HFC-32 is, in association with HFC-125, a component of the refrigerant mix used in stationary air
205 conditioning in substitution of the ozone depleting HCFC-22. Due to the availability of observation
206 data from at least two stations starting from 2008, the inversion covers a 7-year period (2008-2014),
207 during which we estimated a yearly average emission from the EGD of 2.3 (± 0.8) Gg yr⁻¹ with a not
208 significant increasing trend of 2.6% yr⁻¹ ($R^2=0.23$). During the common period 2008-2014 our
209 average emission flux is in a fair agreement with the one given by UNFCCC (2.1 Gg yr⁻¹). On the
210 contrary, the analysis of the emission trend highlights an important discrepancy between the
211 inversion (2.6% yr⁻¹) and the UNFCCC database (13.3% yr⁻¹, $R^2=1.0$). EDGAR reported much
212 lower emission fluxes (0.5 Gg yr⁻¹ on average), suggesting incompleteness in the activity data for
213 the inventory compilation. As a further comparison, our estimates of HFC-32 for 2012 represent
214 13.6% of the global emissions calculated by O'Doherty et al. (2014) for the same year. Since the
215 population of the EGD represents about the 7% of global population, this result implies that EGD
216 per-capita emissions are about two times larger than the global average for 2012 given by
217 O'Doherty et al. (2014).

218

219 *HFC-125*

220 For the cooling agent (stationary air conditioning) and fire extinguisher HFC-125 inversion results
221 are available over 2003-2014. We estimated yearly average emission of 6.9 (± 2.4) Gg yr⁻¹ and an
222 increasing trend of 5.0% yr⁻¹ ($R^2=0.65$). Our estimates are on average ca. 20% higher than
223 UNFCCC and EDGAR, even if both inventories report emissions within the uncertainty of the
224 inversion. Larger differences are observed in the trend comparison. Once again, the emission trend
225 derived by the inversion is slower than that observed for UNFCCC (9.1%, $R^2=0.99$). EDGAR data
226 show a good agreement with UNFCCC. Brunner et al. (2012), considering a smaller domain
227 including twelve European countries (corresponding to our EGD with NEE, SCA and SEE
228 subtracted), obtained for the same compound emissions of 3.9 (± 0.2) and 4.5 (± 0.2) Gg yr⁻¹, in 2006
229 and 2009, respectively, using a different modelling approach and a different station geometry. Such
230 values compare with our estimates, for the same years and domain of Brunner et al. (2012), of 4.5
231 (± 1.3) and 4.6 (± 1.3) Gg yr⁻¹.

232

233 *HFC-134a*

234 For HFC-134a we estimated emissions over the period 2003-2014 that are on average 20.1 (± 6.3)
235 Gg yr⁻¹, making HFC-134a the most emitted HFC in Europe. This value is 25% lower than
236 UNFCCC. Emissions reported by European countries to UNFCCC are likely to be affected by an
237 overestimate of the emission factors (EFs) used in some countries in order to compile the emission
238 inventories (Lunt et al., 2015). It is interesting to note how annual emissions of the three databases
239 are essentially coincident in the first part of the record, and then diverge rapidly after 2006. In
240 Europe, HFC-134a is mainly (48-59% in 2010) used as refrigerant fluid in Mobile Air Conditioning
241 (MAC) systems. Our results suggest, in agreement with Say et al. (2016), an overestimation of
242 HFC-134a EFs. The European MAC directive 2006/40/EC, entered into force in 2008, implies the
243 rejection of new type of vehicles fitted with MACs containing i) gases with a GWP higher than 150
244 or ii) leaking more than 40 or 60 grams of the refrigerant per year in the one or dual evaporator
245 systems, respectively. Since car manufacturers were not ready to substitute HFC-134a with lower
246 GWP fluids, it is reasonable to assume that the compliance with the MAC directive has been
247 pursued through the reduction of leaking, not followed by a consistent adjustment of the EFs.
248 Annual emissions derived by the inversion (-1.1% yr⁻¹, $R^2=0.24$) do not show any statistically
249 significant trend. The trend exhibited by UNFCCC data is 4.2% yr⁻¹ ($R^2=0.94$). EDGAR, which
250 used the growth trend 1995-2005 of the car manufacturing as proxy for HFC-134a trend for the air
251 conditioning of cars, shows even higher emission fluxes and trends.

252

253 *HFC-143a*

254 The high GWP value of HFC-143a makes reliable estimates of its emissions particularly relevant,
255 since it represents the main single contributor to CO₂-eq normalized emissions in Europe. HFC-
256 143a is mainly used as a working fluid component in refrigerant blends for low- and medium-
257 temperature commercial refrigeration systems (O'Doherty et al. 2014). The inversion estimated
258 HFC-143a average emission of 5.8 (± 2.0) Gg yr⁻¹ over 2006-2014. These figures are on average 7%
259 higher than UNFCCC data, which are anyway within the error bar of the top-down estimates. The
260 annual inversion estimates exhibit a trend (3.0% yr⁻¹, $R^2=0.38$) slower with respect to the quasi-
261 linear trends of UNFCCC (5.1% yr⁻¹, $R^2=0.92$). Also in this case the EDGAR data exhibit a higher
262 average emission flux and a faster emission trend. As a further comparison, analogously to HFC-32,
263 we put our EGD estimates in a global perspective, comparing the HFC-143a inversion estimates for
264 2012 (7.1 Gg yr⁻¹) with the global ones (23.3 Gg yr⁻¹) given by O'Doherty et al. (2014). As stated
265 above, considering that the population of the EGD represents about the 7% of global population,
266 this result implies that EGD per-capita emissions are more than four times larger than the global
267 average for 2012 (O' Doherty et al., 2014).

268

269 *HFC-152a*

270 In 2003-2014 yearly EGD emissions of the blowing agent HFC-152a are on average 4.1 (± 1.8) Gg
271 yr^{-1} , with a decreasing trend of $-4.6\% \text{ yr}^{-1}$ ($R^2=0.49$). Our estimates are in reasonable agreement
272 with UNFCCC national reports (3.7 Gg yr^{-1}) that always fall within the uncertainty of the inversion.
273 UNFCCC emissions do not show any significant trend ($-1\% \text{ yr}^{-1}$, $R^2=0.25$). In contrast, EDGAR
274 data tend to estimate higher emission fluxes and an increasing trend.

275 HFC-152a top-down emission estimates from similar studies, obtained following different
276 approaches, show an overall fair agreement with our results. Brunner et al. (2012) estimated
277 emissions of 2.0 (± 0.2) and 1.9 (± 0.2) Gg yr^{-1} for 2006 and 2009, respectively. Such emissions refer
278 to the twelve European countries domain corresponding to our EGD with NEE, SCA and SEE
279 subtracted. When considering the same geographic domain our estimates are 2.3 ± 0.8 and 1.8 ± 0.6
280 Gg yr^{-1} , respectively. Simmonds et al. (2016) estimated European emissions of 6.4 (5.2–7.5) and
281 5.2 (4.1–6.4) Gg yr^{-1} in 2010–2012 and 2007–2009, respectively to be compared with 4.2 ± 1.8 and
282 4.0 ± 1.8 obtained through our method in the same three-years for an approximately coincident
283 domain.

284

285 *HFC-227ea*

286 Yearly emissions of HFC-227ea, a fire retardant and a propellant in metered-dose inhalers, have
287 been estimated from 2008 to 2014 at an average value of 0.41 (± 0.22) Gg yr^{-1} , with a positive trend
288 of $4.4\% \text{ yr}^{-1}$ ($R^2=0.59$). It should be noted that, in this case, annual average emissions estimated
289 through the inversion are affected by an uncertainty of 45% (higher than the 35% uncertainty
290 resulting from the model), because of the high uncertainty in the measurement due to the very low
291 atmospheric mixing ratios of HFC-227ea. Our EGD inversion results are in a very good agreement
292 with the UNFCCC annual emission values (average 0.39 Gg yr^{-1}). Analogously, we found a fair
293 agreement also in the emission trend (5.6% , $R^2=0.99$) of UNFCCC. EDGAR reports a steep
294 increasing trend not confirmed by the inversions, with emission values one order of magnitude
295 larger than the top-down estimates. Moreover an outlier in 2009 indicates an error (related to the
296 Austria macro-area). The good agreement of our inversion results with the UNFCCC records
297 suggests that the large underestimation of global UNFCCC reports found by Vollmer et al. (2011)
298 based on a global inversion, is probably due to regions other than Europe, where many countries do
299 not report to the UNFCCC.

300

301 *HFC-236fa*

302 HFC-236fa is a fire retardant and a coolant in specialized applications. Average estimated
303 emissions over 2008-2014 are $0.02 (\pm 0.01)$ Gg yr⁻¹, with a trend of $3.6\% \text{ yr}^{-1}$ ($R^2=0.30$). As for HFC-
304 227ea, for this compound the average annual emission is affected by a high uncertainty (54%) due to
305 the measurement uncertainty. Our results exceed both UNFCCC and EDGAR by about 50%. This
306 suggests that there could be a deficit in the UNFCCC and EDGAR inventories, with very few
307 countries reporting their emissions. Our inversion values are significantly larger than projections
308 given by the IPCC (2005) that estimated for 2015 global emissions of 0.05 Gg yr^{-1} , corresponding
309 to about twice the total emissions from EGD, suggesting an important gap in the reported global
310 emissions. Such an underestimation is also reported in Vollmer et al. (2011), which estimated
311 global HFC- 236fa emissions of 0.018 Gg yr^{-1} in the 2008–2010 period.

312

313 *HFC-245fa*

314 The main market for HFC-245fa is in North America, where it is used for polyurethane structural
315 foam blowing (UNEP-TEAP, 2010). We estimated average EGD HFC-245fa emissions over the
316 period 2008-2014 of $0.74 \pm 0.33 \text{ Gg yr}^{-1}$ and a trend of $-3.0\% \text{ yr}^{-1}$ ($R^2 = 0.28$). The UNFCCC
317 database is in a very good agreement over the common period 2008-2014. On the contrary, EDGAR
318 exhibits a positive trend of 18.9% ($R^2 = 1.0$).

319

320 *HFC-365mfc*

321 HFC-365mfc is mainly used for polyurethane structural foam blowing and, to a minor extent, as a
322 blend component for solvents. According to the inversion results, HFC-365mfc emissions from the
323 EGD over 2005-2014 are on average 1.2 Gg yr^{-1} (± 0.6) a value that is three times that given by the
324 UNFCCC (0.4 Gg yr^{-1}). Emissions estimated by the inversion, affected by an uncertainty of 50%
325 because of the low atmospheric mixing ratios of HFC-365mfc, do not show any significant trend ($-$
326 $2.3\% \text{ yr}^{-1}$, $R^2 = 0.24$), whereas UNFCCC data exhibit a decreasing trend of $-4.0\% \text{ yr}^{-1}$ ($R^2=0.7$).
327 EDGAR emission fluxes are closer to UNFCCC reports but with a positive emission trend. As
328 HFC-365mfc is predominantly released in Europe (Stemmler et al., 2007) with negligible emissions
329 from USA and East Asia (Vollmer et al., 2011), and the bottom-up estimates seem to significantly
330 underestimate emissions, it is important to constrain the intensity and distribution of emissions of
331 this growing compound from the EGD.

332

333 *Aggregated emissions of nine HFCs*

334 The last panel in Figure 1 (TOTAL), reports the aggregated emissions for the nine HFCs expressed
335 in Gg-CO₂-eq·yr⁻¹. Considering the time period in which the inversion results are available for nine

336 HFCs (2008-2014), average emissions are 84.2 (± 28.0) Tg-CO₂-eq·yr⁻¹ compared with the average
337 emission fluxes in the UNFCCC database of 95.1 Tg-CO₂-eq·yr⁻¹, resulting in a difference of 13%
338 between the two datasets.

339 This is in agreement with what reported for Annex I countries in a recent study by Lunt et al.
340 (2015), who used AGAGE and NIES observations combined with a hierarchical Bayesian
341 framework to derive global emissions of five HFCs (HFC-32, HFC-125, HFC-134a, HFC-143a,
342 HFC-152a) during 2010-2012. The authors found that, as in our European study, discrepancies
343 between the top-down and bottom-up estimates of the single compounds were balanced when
344 considering the aggregated emissions.

345 However, it is important to underline how, despite the agreement obtained on a yearly basis
346 between the aggregated inversion results and the aggregated UNFCCC national reports, the
347 temporal pattern is different. Whereas the UNFCCC reports show a smooth (monotonic) behaviour,
348 our results exhibit annual variations matching the sales records as reported by UNFCCC, that show
349 for the main HFCs a slight sales increase in 2007-2008 and a 10% sharp decline in 2009, due to the
350 economic crisis, followed by a new increase in 2010, the last year for which sales data are available
351 (Schwartz et al., 2011). Consequently, our results do not show any statistically significant trend in
352 the emissions (0.7% yr⁻¹, R²=0.04), whereas according to UNFCCC, European HFC emissions are
353 significantly ($\alpha=0.01$) increasing by 4.0% yr⁻¹ (R²=0.94) over the period 2008-2014. This finding is
354 particularly relevant for the elaboration of projection scenarios for future HFC emissions. The
355 comparison with EDGAR shows a disagreement both in average emissions, which are 35% higher
356 than the inversion, and in the trend, with EDGAR reporting a significant ($\alpha=0.01$) emission trend of
357 7.3% yr⁻¹ (R²=0.99).

358
359 To summarise, we observed that based on the inversion results only three (HFC-125, HFC-152a and
360 HFC-227ea) out of the nine HFCs considered exhibit a significant ($\alpha = 0.01$) trend over the studied
361 period. In particular, despite the good agreement between the estimated annual aggregated
362 emissions and the UNFCCC aggregated reports, the former do not exhibit any significant trend,
363 differently than UNFCCC and EDGAR time series, which show a marked increasing trend.

364
365 We also calculated the percentage contribution of the single HFCs to the total EGD emissions,
366 reported both as percentage of the total mass emitted in Gg yr⁻¹ and percentage of Gg-CO₂-eq·yr⁻¹.
367 Pie charts in Figure 2 show the percent contribution of each of the nine compounds here considered
368 to EGD HFC aggregated emissions. Percentages are given for the period 2008-2014, when top-
369 down estimates for all the nine HFCs are available. Since the relative share is not changing

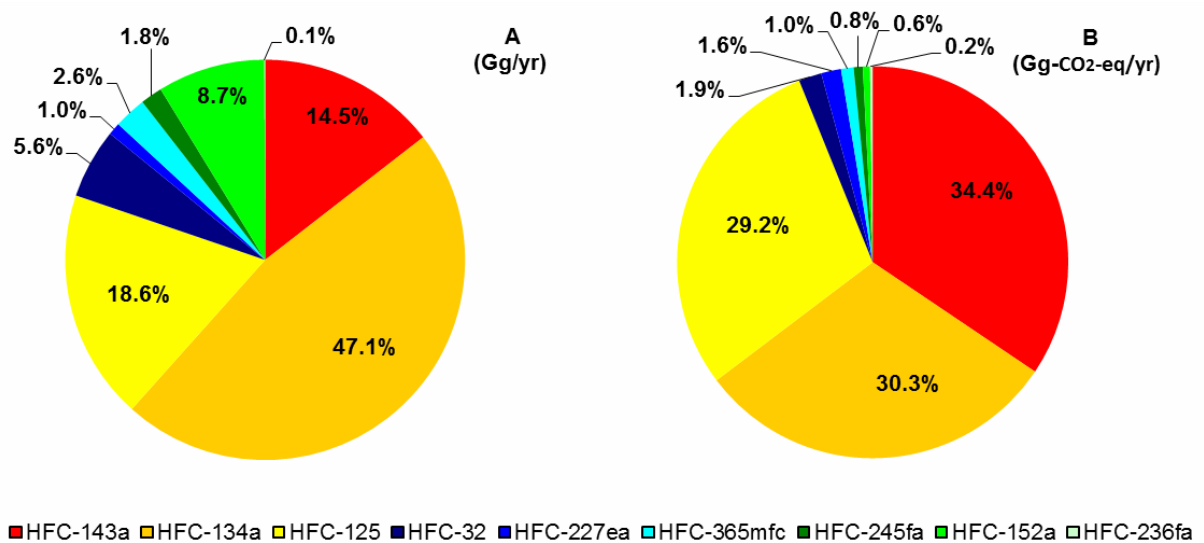
370 significantly from year to year, average values can be considered representative for the entire
 371 period.

372

373 When reporting emissions in Gg-CO₂-eq·yr⁻¹ (Fig.2B), the relative contribution of the single HFCs
 374 is completely different with respect to the mass emitted (Fig. 2A), because of the “weighting” with
 375 different GWP values associated to the various compounds (see Table 1). Using this metric HFC-
 376 143a becomes the compound that contributes more than one third over the total, going from the
 377 14.5% of the total Gg yr⁻¹ to the 34.4% of the total Gg-CO₂-eq·yr⁻¹, while the HFC-134a
 378 contribution drops from 47.1% of the total Gg yr⁻¹ to 30.3% of the total Gg-CO₂-eq·yr⁻¹.
 379 Analogously, the HFC-125 relative share increases from 18.6 to 29.2%, while HFC-32 relative
 380 share drops from 5.6 to 1.9%. Overall, these four HFCs that are used in refrigerant blends account
 381 for 95.8% of the total EGD Gg-CO₂-eq emissions.

382

383



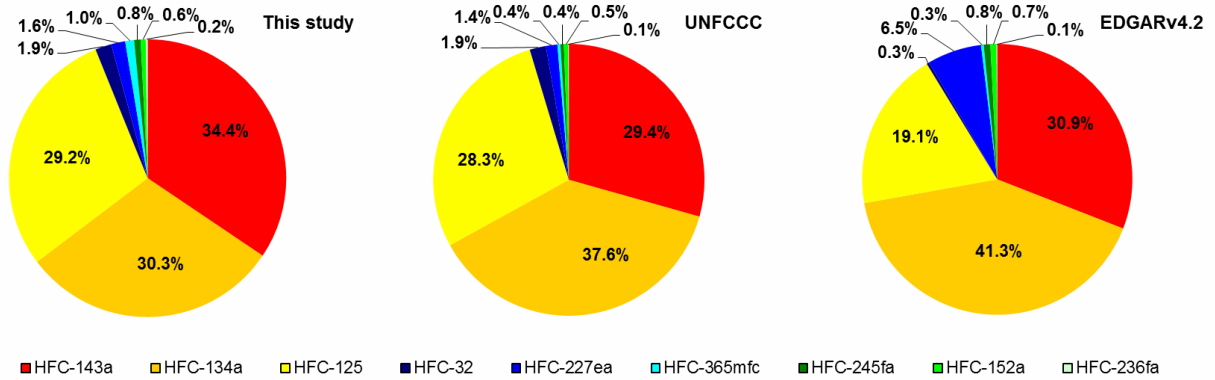
384

385 Figure 2. Averaged relative share of each compound considered in this study to overall HFC emissions from
 386 Europe over 2008-2014. A) percentage of the total emissions in Gg·yr⁻¹; B) percentage of the total emissions
 387 in Gg-CO₂-eq·yr⁻¹.
 388

389 A comparison of percent contribution to Gg-CO₂-eq·yr⁻¹ of emissions derived from the inversion
 390 and those reported by UNFCCC and EDGAR is given in Figure 3. Note that for the inversion
 391 results and UNFCCC data we refer to 2008-2014, whereas for EDGAR we refer to the period 2008-
 392 2010. A reasonable agreement is found for the three most emitted HFCs, whose aggregated
 393 emissions are 95.8 %, 97.2% and 91.6% as from the inversion, UNFCCC and EDGAR,

394 respectively. Differences are mainly due to the under-estimation of HFC-143a and over-estimation
 395 of HFC-134a in the bottom-up inventories with respect to the inversion results. A major
 396 discrepancy is found in relation to EDGAR estimates of HFC-227ea that are five times larger than
 397 the other two data-sets.

398



399

400 Figure 3. Relative share, in Gg-CO₂-eq·yr⁻¹, of nine HFCs to the total European HFC emissions: comparison among
 401 inversion estimates (2008-2014), UNFCCC (2008-2014) and EDGARv4.2FT2010 (2008-2010).

402

403 3.2 Spatial distribution of HFC emissions from the European Geographic Domain.

404 As noted in previous studies (Lunt et al., 2015), it is important to derive emission estimates at
 405 national scales in order to better understand the discrepancies in the UNFCCC reports, evaluate the
 406 reliability of EFs used by various countries and monitor the effectiveness of climate policy
 407 directives.

408 In this section we analyse the spatial distribution of emissions of the nine HFCs considered within
 409 twelve macro-areas in the EGD. In order to allow a comparison with the bottom-up inventories
 410 available, such analysis concerns the average emissions during period 2008-2014, when emissions
 411 for the nine HFCs have been estimated. Emissions from twelve macro-areas of nine HFCs are
 412 reported in Figure 4. Macro-areas acronyms are reported in Figure 4 caption.

413 For HFC-32, according to this study, the main emitters in the EGD are FR, ES-PT and IT, followed
 414 by UK and NEE that together account for the 75% of the EGD emissions. Despite a difference of
 415 only 10% between the total estimated amount of emitted HFC-32 from twelve macro-areas and the
 416 corresponding UNFCCC country reports, going to the single macro-area level significant
 417 discrepancies are found. We estimate for ES-PT, UK, NEE and SEE emissions that are only about
 418 half of the UNFCCC ones, whereas the UNFCCC number of IT accounts only ca. 50% of the
 419 inversion estimates. As already shown by the previous analysis, EDGAR reports HFC-32 emissions

420 that are ca. 25% of the inversion estimates for all macro-areas except DE, where a very good
421 agreement is found.

422 For HFC-125 the main emitters in our study are FR, ES-PT, IT, UK, and NEE, accounting for 72%
423 of total EGD emissions. The agreement with UNFCCC is within the error bars of the inversion for
424 most of the macro-areas, except ES-PT, UK and NEE reporting higher emissions with respect to our
425 estimates. A fair agreement is observed with EDGAR, with the exception of DE and BE-NE-LU,
426 for which the EDGAR estimated emissions are approximately double the inversion results, and ES-
427 PT that according to the inventory emits less than half the inversion estimates.

428 74% of HFC-134a EGD emissions in our study are attributed to FR, UK, IT, DE and ES-PT. As
429 discussed in the previous section, in general UNFCCC reports higher emissions than our results for
430 all the macro-areas, and especially in NEE, UK and DE. The only exception is Italy that reports
431 emissions that are two thirds of the estimated ones. Indeed, the HFC-134a EFs used by the Italian
432 National Institute for Environmental Protection (Istituto Superiore per la Protezione e la Ricerca
433 Ambientale, ISPRA) have been regularly updated after confrontation with the motor manufacturers'
434 association and are lower than those suggested in the IPCC guidelines (ISPRA, personal
435 communication, 2016). As for the EDGAR inventory, we observe a general overestimation,
436 especially in DE, NEE and SEE.

437 The main emitting macro-areas of HFC-143a in our study are FR, ES-PT, IT, UK, NEE and DE.
438 These six macro-areas account for more than 80% of total EGD emissions. The agreement with
439 UNFCCC is very good, with DE and NEE report values slightly outside the uncertainty of the
440 inversion. The agreement between the inversion and EDGAR is generally good with the exception
441 of DE, for which EDGAR reports emissions that are more than double than the inversion. The
442 agreement between the top-down and bottom-up estimates is particularly relevant, given the high
443 GWP value of HFC-143a, which is the major HFC emitted in terms of CO₂-eq.

444 The main emitter of HFC-152a in our study is IT, accounting alone for 20% of total EGD
445 emissions, followed by SEE, FR, NEE, and DE (total contribution 70%). The agreement with
446 UNFCCC is generally fair for all macro-areas, with two major exceptions: IT does not report any
447 emission to UNFCCC whereas SEE reports emissions 2.5 times larger than the inversion. The
448 discrepancy with UNFCCC is likely to be due to the incompleteness of reported emissions as a
449 consequence of a limited number of producers and confidentiality considerations. For this reason,
450 some countries report to UNFCCC HFC-152a emissions aggregated with other HFCs in the
451 "unspecified mix" category (Simmonds et al., 2015). The emission overestimates in EDGAR are
452 essentially due to FR, DE and UK.

453 In our study HFC-227ea is mainly emitted by FR, UK, DE, ES-PT and IT (overall contribution
454 77%). We observe good agreement with UNFCCC country reports, while EDGAR data for all
455 macro-areas are at least three times larger than the inversion results.

456 Major emitters of HFC-236fa in our study are NEE, ES-PT and DE (contributing the 71% of the
457 EGD emissions) that are also the only macro-areas in the EGD for which UNFCCC and EDGAR
458 data are available. The agreement between our estimates and the bottom-up inventories is
459 satisfactory only for the NEE macro-area.

460 In our study IT, ES-PT, FR, UK and DE account for 71% of HFC-245fa EGD emissions. The very
461 good agreement between the inversion estimates and UNFCCC at the EGD scale does not apply at
462 the single country scale, where UNFCCC reports larger emissions from IT and lower emissions
463 from ES-PT and UK. In addition, UNFCCC reports for seven macro-areas in the EGD are lacking.
464 The EDGAR inventory on average reports emissions larger than the inversion, in particular, for DE
465 and ES-PT.

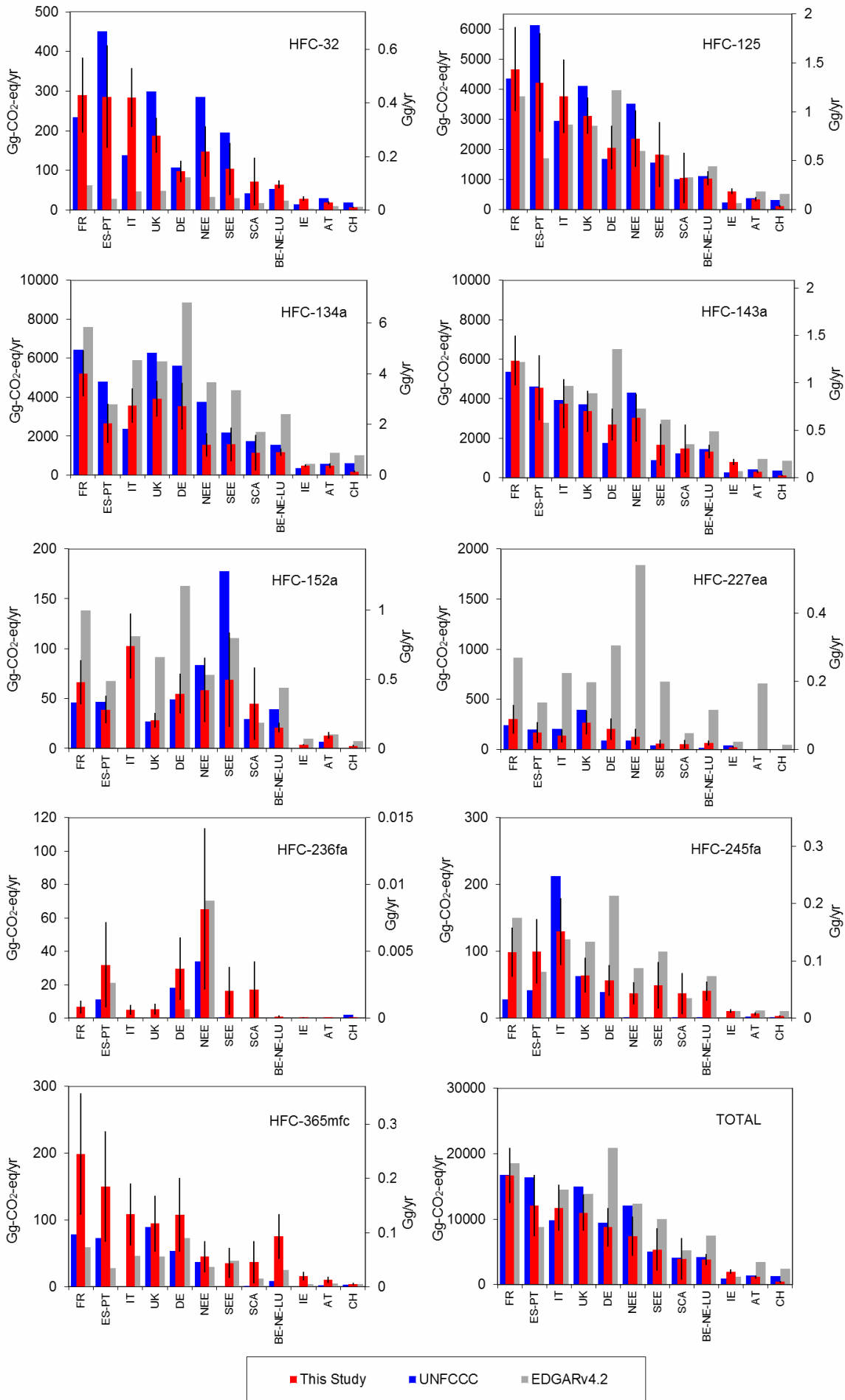
466 In our study HFC-365mfc is mainly emitted by FR and ES-PT that, together with IT, DE and UK,
467 emit 75% of the total EGD. UNFCCC reports emissions that are only one third of the inversion
468 estimates at the EGD scale. This discrepancy is due to the lack of reporting of five macro-areas and
469 the remaining ones are greatly underestimated with the exception of UK and NEE. The EDGAR
470 database reports for this compound emissions which are significantly lower than the inversion,
471 especially for ES-PT, FR, IT, UK.

472 Despite some large discrepancies in selected macro-areas and/or compounds, when converting
473 emissions in CO₂-eq again the aggregated HFC estimated emissions from the twelve macro-areas
474 show a fair agreement with the bottom-up inventories. In particular UNFCCC data are within the
475 error bar of the inversion for most of the macro-areas, whereas in the comparison with EDGAR
476 some discrepancies are observed with DE, BE-NE-LU and SEE inventory exceeding the inversion
477 results.

478

479

480



482 Figure 4. Average emissions during 2008-2014 of nine HFCs from twelve macro-areas in the European Geographic
483 Domain. Red, this study; Blue, UNFCCC; Grey, EDGARv4.2FT2010. Macro-areas, listed according to their aggregated
484 (TOTAL) emission intensity are: FR (France); UK (United Kingdom); ES-PT (Spain, Portugal); IT (Italy); DE
485 (Germany); NEE (Poland, Czech Republic, Slovakia, Lithuania, Latvia, Estonia, Hungary, Romania, Bulgaria); SCA
486 (Norway, Sweden, Finland, Denmark); SEE (Slovenia, Croatia, Serbia, Bosnia-Herzegovina, Montenegro, Albania,
487 Greece); BE-NE-LU (Belgium, The Netherlands, Luxembourg), IE (Ireland); AT (Austria); CH (Switzerland).

488

489 3.3 Per-capita emissions from the European Geographic Domain.

490 Considering the strong inhomogeneity in terms both of area, population and HFC production
491 facilities of the twelve macro-areas under investigation, per-capita emissions have been calculated.
492 They are representative of the sum of emissions due to industrial processes (point source emissions)
493 and individual consumption (diffusive emissions).

494 Figure 5 shows the geographic distribution of per-capita emissions, given in $\text{kg-CO}_2\text{-eq}\cdot\text{yr}^{-1}$
495 $\cdot\text{inhabitants}^{-1}$, from twelve macro-areas in the EGD. Columns A, B and C refer to the inversion
496 estimates (averaged over 2008-2014), UNFCCC (averaged over 2008-2014) and EDGAR
497 (averaged over 2008-2010), respectively.

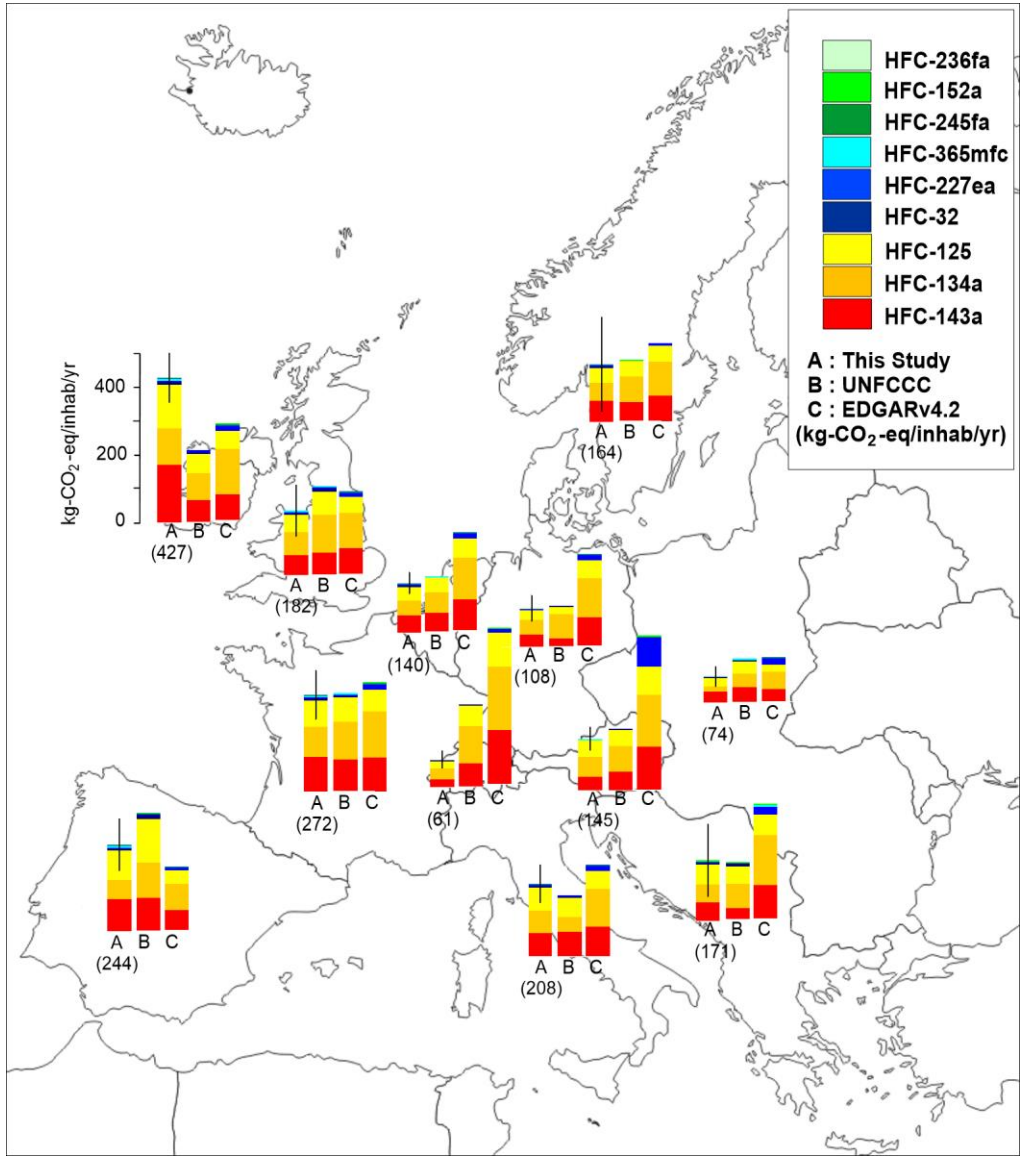
498 The per-capita value for which we found the largest deviation from the EGD average emission of
499 $183 \text{ kg-CO}_2\text{-eq}\cdot\text{yr}^{-1}\cdot\text{inhabitants}^{-1}$ is that referred to Ireland (IE), where we estimated a much higher
500 value of $427 \text{ kg-CO}_2\text{-eq}\cdot\text{yr}^{-1}\cdot\text{inhabitants}^{-1}$. Emissions from IE larger than the average are also
501 reported in the bottom-up inventories. Such deviation from the average value is likely to be due to
502 the weight of industrial emissions that become more relevant in a low-populated area.

503 Further emissions above the European average, in the range $208\text{-}272 \text{ kg-CO}_2\text{-eq}\cdot\text{yr}^{-1}\cdot\text{inhabitants}^{-1}$,
504 have been estimated for FR, ES-PT and IT whereas for UK, SEE, SCA, AT, BE-NE-LU, DE and
505 NEE we estimated below average emissions ranging from 74 to $183 \text{ kg-CO}_2\text{-eq}\cdot\text{yr}^{-1}\cdot\text{inhabitants}^{-1}$.

506 Finally, for the CH area we estimated per-capita emissions significantly lower than the European
507 average and lower than the bottom-up inventories. However, it must be underlined that the model
508 allocation of emissions from a relatively small area is affected by the so-called border problem, and
509 is therefore less reliable.

510 In order to assess the contribution of industrial emissions to per-capita ones, it might be useful to
511 analyse fluxes reported to the European Pollutant Release and Transfer Register (E-PRTR). The E-
512 PRTR is a Europe-wide register that provides environmental data from 30,000 industrial facilities
513 covering 65 economic activities within 9 industrial sectors in EU member states, as well as in
514 Iceland, Liechtenstein, Norway, Serbia and Switzerland and reports HFC atmospheric emissions
515 higher than 100 kg yr^{-1} . Based on E-PRTR data, aggregated HFC emissions in mass correspond to

516 circa one thirtieth of the inversion estimates. Unfortunately, the European Regulation CE/166/2006
 517 requires this inventory to include HFC aggregated emissions reported not in CO₂-eq but in weight
 518 mass, a metric that does not allow a comparison with the inversion results, nor does it allow an
 519 assessment of the actual impact of industrial emissions to the total radiative forcing due to HFCs.



520
 521 Figure 5: Per-capita emissions from twelve macro-areas in the European Geographic Domain. Emissions, given in kg-
 522 CO₂-eq·y⁻¹·inhabitants⁻¹, are averaged over 2008-2014 for the inversion results (columns A) and the IPCC country
 523 reports (columns B). EDGAR data (columns C) are averaged over 2008-2010.

524
 525 The average EGD per-capita CO₂ equivalent emissions derived through the inversion resulted to be
 526 up to four times larger than the average global ones, calculated from top-down estimates reported
 527 by Rigby et al. (2014) and higher than Chinese per-capita emissions based on Fang et al. (2016), but
 528 lower than those estimated by Lunt et al. (2015) from the West USA, (representing the 21 % of U.S.
 529 population). A summary of such comparison is reported in Table 2.

531 Table 2. Per-capita average HFC emissions in 2010-2012 derived through top-down methods across different world
 532 areas. Emissions are given in $\text{kg-CO}_2\text{-eq}\cdot\text{y}^{-1}\cdot\text{inhabitants}^{-1}$.
 533

$\text{kg-CO}_2\text{-eq}\cdot\text{y}^{-1}$ $\cdot\text{inhabitants}^{-1}$	EGD (this study)	China (Fang et al. 2016)	West USA (Lunt et al. 2015)	Global (Rigby et al. 2014)
HFC-32	3.4±1.2	4.0	3.4	1.5
HFC-125	55±19	15	88	15
HFC-134a	53±18	22	140	31
HFC-143a	59±21	8.7	83	14
HFC-152a	1.1±0.4	1.6	9.0	1.0
HFC-227ea	3±1	NA	NA	1.3
HFC-236fa	0.3±0.1	NA	NA	0.2
HFC-245fa	1.2±0.4	NA	NA	0.9
HFC-365mfc	1.9±0.7	NA	NA	0.4

534

535 4. Conclusions

536

537 This study captures the current status of HFC emissions at the European scale at a time immediately
 538 preceding their phase-down, as agreed during the 28th Meeting of the Parties to the Montreal
 539 Protocol (Kigali, October 2016). The top-down approach used in this study allowed us to derive
 540 emission fluxes of nine HFCs based on long-term, high-frequency observations. It is a very
 541 powerful tool for integrating and supporting existing emission data available in the bottom-up
 542 inventories that are prone to be affected by the use of different emission factors or absences in the
 543 national reports. The sensitivity analyses have shown that the inversion results are robust and
 544 produce stable results despite the high variability of input data and inversion settings.

545

546 *Spatial distribution:* The analysis of the spatial distribution of HFC emissions within the European
 547 geographic domain allowed us to identify four macro-areas, FR, UK, ES-PT and IT, as the main
 548 emitting areas responsible for the 61% of aggregated emissions from 2008 to 2014. According to
 549 UNFCCC and EDGAR the four macro-areas represent the 60% (2008-2014) and 47% (2008-2010)
 550 of total emissions, respectively. Important discrepancies are highlighted when considering the
 551 spatial distribution, for example the IT macro-area being the main emitter of HFC-152a, whereas in
 552 the UNFCCC database no emissions are reported.

553

554 *Single compound emissions:* The comparison with the UNFCCC database was done over 2003-
 555 2014 or shorter periods, according to the considered compounds. Our results are in fair agreement
 556 for most of the compounds. Percent variations, calculated as (inversion results –

557 UNFCCC)/inversion results, for HFC-125, HFC-143a, HFC-152a and HFC-227ea are lower than
558 10%. HFC-32 and HFC-134a are estimated by the inversion are lower than UNFCCC by -19% and
559 23%, respectively. Such values are always within the inversion uncertainty. A larger discrepancy
560 was found for HFC-236fa, HFC-245fa and HFC-365mfc (65%, 39% and 62%, respectively). The
561 comparison with EDGAR (2003-2008 or shorter periods according to the different compounds)
562 reveals that this inventory underestimates emission data for HFC-32 and HFC-365mfc but
563 overestimates emission data for HFC-227ea. Inversion estimates for the compound with the highest
564 emissions, HFC-134a, are 50% lower than the inventory and with a markedly different trend,
565 suggesting a shortcoming in the activity data as non-representative proxy for the emission trends for
566 this compound affecting bottom-up estimates.

567

568 *Aggregated emissions:* Despite the several discrepancies when considering the single compounds,
569 an overall agreement is found when comparing aggregated data. We estimated that European
570 aggregated emissions from 2008 to 2014, the period in which the inversions have been run for all
571 the nine HFCs, and considering their 100-yr GWP, are on average 84.2 ± 28.0 Tg-CO₂-eq·yr⁻¹
572 against the 95.1 Tg-CO₂-eq·yr⁻¹ reported by UNFCCC in the same period. These results support, as
573 far as Europe is concerned, the findings by Lunt et al. (2015). These authors observed a substantial
574 agreement between emissions from Annex I countries inferred by atmospheric observations and
575 those reported to UNFCCC, suggesting that the existing gap between global top-down and bottom-
576 up estimates (Rigby et al., 2014) should be essentially due to non-reporting countries. However, the
577 discrepancies between the UNFCCC country reports and the inversion results evidenced by this
578 study when considering the single countries and the single compounds confirm that the agreement
579 is more due to a cancellation of errors rather than to the accuracy in compiling the emission
580 inventories. Thus, our results could help in identifying which compounds and macro-areas would
581 need more robust estimates of emission fluxes.

582 Further regional studies from other Annex I countries are necessary in order to better constrain the
583 HFC global budget. In addition, the differences found when comparing the emission trends as
584 derived by the inversion with those reported to UNFCCC could affect the effectiveness of the
585 adopted climate policies.

586

587 **Acknowledgments**

588 We acknowledge the AGAGE science team as well as the station personnel at all stations for their
589 continuous support in conducting in situ measurements. M. Maione acknowledges useful
590 discussions with Stephen A. Montzka and David W. Fahey. At Jungfraujoch measurements are

591 conducted under the HALCLIM project funded by the Swiss Federal Office for the Environment
592 (FOEN). We also thank the International Foundation High Altitude Research Stations Jungfrauoch
593 and Gornergrat (HFSJG) for support. The instrument operation at Mace Head is supported by the
594 Department of Energy and Climate Change (DECC, UK), at Zeppelin by the Norwegian
595 Environment Agency. The logistic at the "O.Vittori" station (Monte Cimone) is supported by the
596 National Research Council of Italy. Activities at Mace Head (Bristol University), Jungfrauoch
597 (Empa), Monte Cimone (University of Urbino), and Zeppelin (NILU) were also supported through
598 InGOS (Integrated Non-CO₂ Greenhouse gas Observing System, European FP-7 Infrastructure
599 project grant agreement 284274). The University Consortium CINFAI (Consorzio Interuniversitario
600 Nazionale per la Fisica delle Atmosfere e delle Idrosfere) supported F. Graziosi grant (RITMARE
601 Flagship Project).

602

603 **References**

604 Bergamaschi, P., Behrend, H., and Jol, A. (Eds.), 2004. Inverse modelling of national and EU
605 greenhouse gas emission inventories – report of the workshop “Inverse modelling for potential
606 verification of national and EU bottom-up GHG inventories” under the mandate of the Monitoring
607 Mechanism Committee WG-1, 23–24 October 2003, JRC, Ispra, 144, EUR 21099 EN/ISBN 92-
608 894-7455-6, European Commission Joint Research Centre, Ispra (IT).

609 Brunner, D., Henne, S., Keller, C. A., Reimann, S., Vollmer, M. K., O'Doherty, S., and Maione, M.,
610 2012. An extended Kalman-filter for regional scale inverse emission estimation. *Atmos. Chem.*
611 *Phys.* 12, 3455-3478.

612 Eckhardt, S., Prata, A. J., Seibert, P., Stebel, K., and Stohl, A., 2008. Estimation of the vertical
613 profile of sulfur dioxide injection into the atmosphere by a volcanic eruption using satellite column
614 measurements and inverse transport modelling. *Atmos. Chem. Phys.* 8, 3881–3897.

615 EDGAR (Emission Database for Global Atmospheric Research), release version 4.2 FT2010, 2011.
616 European Commission, Joint Research Centre (JRC)/Netherlands Environmental Assessment
617 Agency (PBL): <http://edgar.jrc.ec.europa.eu>.

618 EU (European Union), 2006. Directive 2006/40/EC of the European parliament and of the council of
619 17 May 2006 relating to emissions from air-conditioning systems in motor vehicles. *Off. J. EU*,
620 L161 (2006), pp. 12–18

621 EU (European Union), 2014. Regulation (EC) No 517/2014 of the European parliament and of the
622 council of 16 April 2014 on fluorinated greenhouse gases and repealing Regulation (EC) No
623 842/2006. *Off. J. EU*, L 150 (2014), pp. 195–230.

624 Fang, X., Velders, G. J. M., Ravishankara, A. R., Molina, M. J., Hu, J., and Prinn, R. G., 2016.
625 Hydrofluorocarbon (HFC) Emissions in China: An Inventory for 2005–2013 and Projections to
626 2050. *Environ. Sci. Technol.*, 50, 2027–2034.

627 Graziosi, F., Arduini, J., Furlani, F., Giostra, U., Kuijpers, L. J. M., Montzka, S. A., Miller, B. R.,
628 O’Doherty, S. J., Stohl, A., Bonasoni, P., and Maione, M., 2015. European emissions of HCFC-22
629 based on eleven years of high frequency atmospheric measurements and a Bayesian inversion
630 method. *Atmos. Environ.* 112, 196-207.

631 Henne, S., Brunner, D., Oney, B., Leuenberger, M., Eugster, W., Bamberger, I., Meinhardt, F.,
632 Steinbacher, M. and Emmenegger, L., 2016. Validation of the Swiss methane emission inventory by
633 atmospheric observations and inverse modelling. *Atmos. Chem. Phys.* 16, 3683-3710.

634 Hu, L., Montzka, S. A., Miller, J. B., Andrews, A. E., Lehman, S. J., Miller, B. R., Thoning, K.,
635 Sweeney, C., Chen, H., Godwin, D. S., Masarie, K., Bruhwiler, L., Fischer, M. L., Biraud, S. C.,
636 Torn, M. S., Mountain, M., Nehrkorn, T., Iuzzkiewicz, J. E., Miller, S., Draxler, R. R., Stein, A. F.,
637 Hall, B. D., Elkins J. W., & Tans P. P., 2015, U.S. emissions of HFC-134a derived for 2008–2012
638 from an extensive flask-air sampling network. *J. Geophys. Res. Atmos.* 120, 801–825.

639 Kim, J., Li, S., Kim, K.-Y., Stohl, A., Mühle, J., Kim, S.-K., Park, M.-K., Kang, D.-J., Lee, G.,
640 Harth, C.M., Salameh, P. K., Weiss, R. F., 2010. Regional atmospheric emissions determined from
641 measurements at Jeju Island, Korea: Halogenated compounds from China. *Geophys. Res. Lett.* 37,
642 L12801.

643 Grealley, B. R., Manning, A. J., Reimann, S., McCulloch, A., Huang, J., Dunse, B. L., Simmonds, P.
644 G., Prinn, R. G., Fraser, P. J., Cunnold, D. M., O’Doherty, S., Porter, L. W., Stemmler, K., Vollmer,
645 M. K., Lunder, C. R., Schmidbauer, N., Hermansen, O., Arduini, J., Salameh, P. K., Krummel, P.
646 B., Wang, R. H. J., Folini, D., Weiss, R. F., Maione, M., Nickless, G., Stordal, F., Derwent, R. G.,
647 2007. Observations of 1,1-difluoroethane (HFC-152a) at AGAGE and SOGE monitoring stations in
648 1994–2004 and derived global and regional emission estimates. *J. Geophys. Res.* 112, D06308.

649 Hurwitz, M.M., Fleming, E.L., Newman, P.A., Li, F., Mlawer, E., Cady- Pereira, K. and Bailey, R.,
650 2015. Ozone depletion by hydrofluorocarbons. *Geophys. Res. Lett.* 42, 8686-8692.

651 IPCC (Intergovernmental Panel on Climate Change), 1990. IPCC First Assessment Report (FAR),
652 Houghton, J.T., Jenkins, G.J., Ephraums, J.J. (eds.). Cambridge University Press, Cambridge, UK,
653 New York, NY, USA and Melbourne, Australia, 410 pp.

654 IPCC (Intergovernmental Panel on Climate Change), 2005. IPCC/TEAP (Technology and
655 Economic Assessment Panel) Special Report on Safeguarding the Ozone Layer and the Global
656 Climate System: Issues Related to Hydrofluorocarbons and Perfluorocarbons. Prepared by
657 Working Group I and III of the Intergovernmental Panel on Climate Change, and the Technology
658 and Economic Assessment Panel, Cambridge Univ. Press, Cambridge, UK, 488 pp.

659 IPCC (Intergovernmental Panel on Climate Change), 2006: 2006 IPCC Guidelines for National
660 Greenhouse Gas Inventories, Prepared by the National Greenhouse Gas Inventories Programme,
661 Eggleston, H.S., Buendia, L., Miwa, K., Ngara, T., Tanabe, K. (eds). Published: IGES, Japan.

662 IPCC (Intergovernmental Panel on Climate Change), 2013: Summary for Policymakers. In: Climate
663 Change 2013: The Physical Science Basis. Contribution of Working Group I to the Fifth
664 Assessment Report of the Intergovernmental Panel on Climate Change [Stocker, T.F., Qin, D.,
665 Plattner, G.-K., Tignor, M., Allen, S.K., Boschung, J., Nauels, A., Xia, Y., Bex, V., Midgley, P.M.
666 (eds.)]. Cambridge University Press, Cambridge, UK and New York, NY, USA.

667 Keller, C. A, Hill, M., Vollmer, M. K., Henne, S., Brunner, D., Reimann, S., O'Doherty, S.,
668 Arduini, J., Maione, M., Ferenczi, Z., Haszpra, L., Manning, A. J., Peter, T., 2012. European
669 Emissions of Halogenated Greenhouse Gases Inferred from Atmospheric Measurements. *Environ.*
670 *Sci. & Technol.* 46, 217-225.

671 Li, S., Kim, J., Kim, K.-R., Mühle, J., Kim, S.-K., Park, M.-K., Stohl, A., Kang, D.-J., Arnold, T.,
672 Harth, C.M., Salameh, P.K., Weiss R. F., 2001. Emissions of Halogenated Compounds in East Asia
673 Determined from Measurements at Jeju Island, Korea. *Environ. Sci. & Technol.* 45, 5668-5675.

674 Lunt, M.F., Rigby, M., Ganesan, A. L., Manning, A. J., Prinn, R. G., O'Doherty, S., Mühle, J.,
675 Harth, C. M., Salameh, P. K., Arnold, T., Weiss, R. F., Saito, T., Yokouchi, Y., Krummel, P. B.,
676 Steele, L., Fraser, P. J., Li, S. Park, S., Reimann, S., Vollmer, M. K., Lunder, C., Hermansen, O.,
677 Schmidbauer, N., Maione, M., Arduini, J., Young, D., Simmonds, P. G, 2015. Reconciling reported
678 and unreported HFC emissions with atmospheric observations. *PNAS* 112, 5927–593.

679 Maione, M., Giostra, U., Arduini, J., Furlani, F., Graziosi, F., Lo Vullo, E., Bonasoni, P., 2013.
680 Ten years of continuous observations of stratospheric ozone depleting gases at Monte Cimone
681 (Italy) - Comments on the effectiveness of the Montreal Protocol from a regional perspective. *Sci.*
682 *Tot. Environ.* 445–446, 155–164.

683 Maione, M., Graziosi, F., Arduini, J., Furlani, F., Giostra, U., Blake, D.R., Bonasoni, P., Fang, X.,
684 Montzka, S.A., O'Doherty, S., Reimann, S., Stohl, A., and Vollmer, M.K., 2014. Estimates of
685 European emissions of methyl chloroform using a Bayesian inversion method. *Atmos. Chem. Phys.*
686 14, 9755-9770.

687 Manning, A. J., O'Doherty, S., Jones, A. R., Simmonds, P. G., Derwent, R. G., 2011. Estimating
688 UK methane and nitrous oxide emissions from 1990 to 2007 using an inversion modeling approach.
689 *J. Geophys. Res.* 116(D2), D02305.

690 Myhre, G., Shindell, D., Bréon, F.-M., Collins, W., Fuglestedt, J., Huang, J., Koch, D., Lamarque,
691 J.-F., Lee, D., Mendoza, B., Nakajima, T., Robock, A., Stephens, G., Takemura, T., Zhang, H.,
692 2013. Anthropogenic and Natural Radiative Forcing. In: *Climate Change 2013: The Physical*
693 *Science Basis. Contribution of Working Group I to the Fifth Assessment Report of the*
694 *Intergovernmental Panel on Climate Change* [Stocker, T.F., Qin, D., Plattner, G.-K., Tignor, M.,
695 Allen, S.K., Boschung, J., Nauels, A., Xia, Y., Bex V., Midgley, P.M. (eds.)]. Cambridge
696 University Press, Cambridge, UK and New York, NY, USA.

697 Miller, B.R., Weiss, R.F., Salameh, P.K., Tanhua, T., Grealley, B.R., Mühle, J., Simmonds, P.G.,
698 2008. Medusa: A sample preconcentration and GC/MS detector system for in situ measurements
699 of atmospheric trace halocarbons, hydrocarbons, and sulphur compounds. *Anal. Chem.* 80, 1536-
700 1545.

701 Miller, B. R., Rigby, M., Kuijpers, L. J. M., Krummel, P. B., Steele, L. P., Leist, M., Fraser, P. J.,
702 McCulloch, A., Harth, C., Salameh, P., Mühle, J., Weiss, R. F., Prinn, R. G., Wang, R. H. J.,
703 O'Doherty, S., Grealley, B. R., Simmonds, P. G, 2010. HFC-23 (CHF₃) emission trend response to
704 HCFC-22 (CHClF₂) production and recent HFC-23 emission abatement measures. *Atmos. Chem.*
705 *Phys.* 10, 7875-7890.

706 Montzka, S. A., Myers, R. C., Butler, J. H. and Elkins, J. W., 1994. Early trends in the global
707 tropospheric abundance of hydrochlorofluorocarbon-141b and 142b, *Geophys. Res. Lett.* 21, 2483–
708 2486.

709 Montzka, S. A., Kuijpers, L., Battle, M. O., Aydin, M., Verhulst, K. R., Saltzman, E. S., Fahey, D.
710 W., 2010. Recent increases in global HFC-23 emissions. *Geophys. Res. Lett.* 37, L02808.

711 Montzka, S.A. and Reimann, S. (lead authors), Engel, A., Krüger, K., O'Doherty, S., Sturges, W.
712 T., Blake, D., Dorf, M., Fraser, P., Froidevaux, L., Jucks, K., Kreher, K., Kurylo, M. J., Mellouki,
713 A., Miller, J., Nielsen, O.-J., Orkin, V. L., Prinn, R. G., Rhew, R., Santee, M. L., and Verdonik, D,
714 2011. Ozone-Depleting Substances (ODSs) and Related Chemicals, Chapter 1 in *Scientific*

715 Assessment of Ozone Depletion: 2010, Global Ozone Research and Monitoring Project-Report No.
716 52, World Meteorological Organization, Geneva, Switzerland, 516p., 1.1-1.108, 2011.

717 Nisbet, E., and Weiss, R., 2010, Top-Down Versus Bottom-Up, *Science*, 328, 1241-1243.

718 O'Doherty, S., Rigby, M., Mühle, J., Ivy, D. J., Miller, B. R., Young, D., Simmonds, P. G.,
719 Reimann, S., Vollmer, M. K., Krummel, P. B., Fraser, P. J., Steele, L. P., Dunse, B., Salameh, P.
720 K., Harth, C. M., Arnold, T., Weiss, R. F., Kim, J., Park, S., Li, S., Lunder, C., Hermansen, O.,
721 Schmidbauer, N., Zhou, L. X., Yao, B., Wang, R. H. J., Manning, A. J., and Prinn, R. G., 2014.
722 Global emissions of HFC-143a (CH₃CF₃) and HFC-32 (CH₂F₂) from in situ and air archive
723 atmospheric observations, *Atmos. Chem. Phys.*, 14, 9249-9258.

724 Prinn R. G., Weiss, R. F., Fraser, P. J., Simmonds, P. G., Cunnold, D. M., Alyea, F. N., O'Doherty,
725 S., Salameh, P., Miller, B. R., Huang, J., Wang, R. H. J., Hartley, D. E., Harth, C., Steele, L. P.,
726 Sturrock, G., Midgley, P. M., McCulloch, A., 2000. A history of chemically and radiatively
727 important gases in air deduced from ALE/GAGE/AGAGE. *J. Geophys. Res.* 105(D14), 17751–
728 17792.

729 Rigby, M., Prinn, R. G., O'Doherty, S., Miller, B. R., Ivy, D. J., Mühle, J., Harth, C. M., Salameh,
730 P. K., Arnold, T., Weiss, R. F., Krummel, P. B., Steele, L. P., Fraser, P. J., Young, D., Simmonds,
731 P. G., 2014. Recent and future trends in synthetic greenhouse gas radiative forcing. *Geophys. Res.*
732 *Lett.* 41, 2623–2630.

733 Say, D., Manning, A. J., O'Doherty, S., Rigby, M., Young, D., Grant, A., 2016. Re-Evaluation of
734 the UK's HFC-134a Emissions Inventory Based on Atmospheric Observations. *Environ. Sci.*
735 *Technol.* 2016, 50, 11129–11136.

736 Schwarz, W., Gschrey, B., Leisewitz, A., Herold, A., Gores, S., Papst, I., Usinger, J., Oppelt, D.,
737 Croiset, I., Pedersen, H., Colbourne, D., Kauffeld, M., Lindborg, A., 2011. Preparatory study for a
738 review of Regulation (EC) No 842/2006 on certain fluorinated greenhouse gases, Final Report
739 Prepared for the European Commission in the context of Service Contract No
740 070307/2009/548866/SER/C4, September 2011.

741 Seibert, P., 2000. Inverse modelling of sulphur emissions in Europe based on trajectories, in:
742 *Inverse Methods in Global Biogeochemical Cycles*, edited by: Kasibhatla, P., Heimann, M.,
743 Rayner, P., Mahowald, N., Prinn, R. G., Hartley, D. E., *Geophysical Monograph* 114, 147–154,
744 American Geophysical Union, ISBN:0-87590-097-6.

745 Seibert, P., 2001. Inverse modelling with a Lagrangian particle dispersion model: application to
746 point releases over limited time intervals, In: *Air Pollution Modeling and its Application XIV*,
747 edited by: Schiermeier, F. A. and Gryning, S.-E., Kluwer Academic Publ., 381–389.

748 Seibert, P. and Frank, A., 2004. Source-receptor matrix calculation with a Lagrangian particle
749 dispersion model in backward mode. *Atmos. Chem. Phys.* 4, 51–63.

750 Shindell, D., Kuylensstierna, J. C. I., Vignati, E., van Dingenen, R., Amann, M., Klimont, Z.,
751 Anenberg, S. C., Muller, N., JanssensMaenhout, G., Raes, F., Schwartz, J., Faluvegi, G., Pozzoli,
752 L., Kupiainen, K., Hoglund-Isaksson, L., Emberson, L., Streets, D., Ramanathan, V., Hicks, K.,
753 Oanh, N. T. K., Milly, G., Williams, M., Demkine, V., and Fowler, D., 2012. Simultaneously
754 Mitigating Near-Term Climate Change and Improving Human Health and Food Security. *Science*
755 335, 183–189.

756 Simmonds, P. G., Rigby, M., Manning, A. J., Lunt, M. F., O'Doherty, S., McCulloch, A., Fraser, P.
757 J., Henne, S., Vollmer, M. K., Mühle, J., Weiss, R. F., Salameh, P. K., Young, D., Reimann, S.,
758 Wenger, A., Arnold, T., Harth, C. M., Krummel, P. B., Steele, L. P., Dunse, B. L., Miller, B. R.,
759 Lunder, C. R., Hermansen, O., Schmidbauer, N., Saito, T., Yokouchi, Y., Park, S., Li, S., Yao, B.,
760 Zhou, L. X., Arduini, J., Maione, M., Wang, R. H. J., Ivy, D., and Prinn, R. G., 2012. Global and
761 regional emissions estimates of 1,1-difluoroethane (HFC-152a, CH₃CHF₂) from in situ and air
762 archive observations, *Atmos. Chem. Phys.* 16, 365-382.

763 Stemmler, K., Folini, D., Ubl, S., Vollmer, M. K., Reimann, S., O'Doherty, S., Grealley, B. R.,
764 Simmonds, P. G., Manning, A. J., 2007. European emissions of HFC-365mfc, a chlorine-free
765 substitute for the foam blowing agents HCFC-141b and CFC-11. *Environ. Sci. Technol.* 41, 1145–
766 1151.

767 Stohl, A., Hittenberger, M., Wotawa, G., 1998. Validation of the Lagrangian particle dispersion
768 model FLEXPART against large scale tracer experiment data. *Atmos. Environ.* 32, 4245–4264..

769 Stohl, A., Forster, C., Frank, A., Seibert, P., Wotawa, G., 2005. Technical note: The Lagrangian
770 particle dispersion model FLEXPART version 6.2. *Atmos. Chem. Phys.* 5, 2461–2474.

771 Stohl, A., Seibert, P., Arduini, J., Eckhardt, S., Fraser, P., Grealley, B. R., Lunder, C., Maione, M.,
772 Mühle, J., O'Doherty, S., Prinn, R. G., Reimann, S., Saito, T., Schmidbauer, N., Simmonds, P. G.,
773 Vollmer, M. K., Weiss, R. F., Yokouchi, Y., 2009. An analytical inversion method for determining
774 regional and global emissions of greenhouse gases: Sensitivity studies and application to
775 halocarbons, *Atmos. Chem. Phys.* 9, 1597-1620.

776 Stohl, A., Kim, J., Li, S., O'Doherty, S., Mühle, J., Salameh, P. K., Saito, T., Vollmer, M. K., Wan,
777 D., Weiss, R. F., Yao, B., Yokouchi, Y., and Zhou, L. X., 2010. Hydrochlorofluorocarbon and
778 hydrofluorocarbon emissions in East Asia determined by inverse modeling, Atmos. Chem. Phys.
779 10, 3545-3560.

780 UNEP (United Nations Environ Programme), 1987. The Montreal Protocol on Substances that
781 Deplete the Ozone Layer (United Nations Environ Programme, Nairobi, Kenya).

782 UNEP-TEAP (United Nations Environ Programme, Technology and Economic Assessment Panel),
783 2010.

784 UNEP (United Nations Environ Programme), 2011. HFCs: A Critical Link in Protecting Climate
785 and the Ozone Layer. United Nations Environment Programme. Nairobi, Kenya , 36pp

786 UNEP (United Nations Environ Programme), 2015a. Proposed Amendment to the Montreal
787 Protocol Submitted by Canada, Mexico and the United States of America. United Nations
788 Environment Programme, Nairobi, Kenya. ISBN:UNEP/OzL.Pro.WG.1/36/3

789 UNEP (United Nations Environ Programme), 2015b. Proposed Amendment to the Montreal
790 Protocol Submitted by European Union and its Member States. United Nations Environment
791 Programme, Nairobi, Kenya. ISBN:UNEP/OzL.Pro.WG.1/36/5

792 UNEP (United Nations Environ Programme), 2015c. Proposed Amendment to the Montreal
793 Protocol Submitted by India. United Nations Environment Programme, Nairobi, Kenya.
794 ISBN:UNEP/OzL.Pro.WG.1/36/4

795 UNEP (United Nations Environ Programme), 2015d. Proposed Amendment to the Montreal
796 Protocol Submitted by Kiribati, Marshall Islands, Mauritius, Micronesia (Federated States of),
797 Palau, Philippines, Samoa and Solomon Islands. United Nations Environment Programme, Nairobi,
798 Kenya. ISBN:UNEP/OzL.Pro.WG.1/36/6

799 UNFCCC (United Nations Framework Convention on Climate Change), 1997: Kyoto Protocol to
800 the United Nations Framework Convention on Climate Change (United Nations, Geneva).

801 UNFCCC (United Nations Framework Convention on Climate Change), 2006: Updated UNFCCC
802 reporting guidelines on annual inventories following incorporation of the provisions of decision
803 14/CP.11. Nairobi, Kenya. <http://unfccc.int/resource/docs/2006/sbsta/eng/09.pdf>

804 Velders, G. J. M., Fahey, D. W., Daniel, J. S., McFarland, M., Andersend, S. O., 2009. The large
805 contribution of projected HFC emissions to future climate forcing, *Proceedings of the National*
806 *Academy of Sciences*, 106, 10949–10954.

807 Velders, G. J. M., Ravishankara, A. R., Miller, M. K., Molina, M. J., Alcamo, J., Daniel, J. S.,
808 Fahey, D.W., Montzka, S. A., and Reimann, S, 2012. Preserving Montreal Protocol Climate
809 Benefits by Limiting HFCs. *Science*, 335, 922-923.

810 Velders, G. J., Fahey, D. W., Daniel, J. S., Andersen, S. O., McFarland, M., 2015. Future
811 atmospheric abundances and climate forcings from scenarios of global and regional
812 hydrofluorocarbon (HFC) emissions. *Atmos. Environ.* 123, 200-209.

813 Vollmer, M. K., Miller, B.R., Rigby, M., Reimann, S., Mühle, J., Krummel, P. B., O'Doherty, S.,
814 Kim, J., Rhee, T. S., Weiss, R. F., Fraser, P. J., Simmonds, P. G., Salameh, P. K., Harth, C. M.,
815 Wang, R. H. J., Steele, L. P., Young, D., Lunder, C. R., Hermansen, O., Ivy, D., Arnold, T.,
816 Schmidbauer, N., Kim, K.-R.I, Grealley, B. R., Hill, M., Leist, M., Wenger, A., Prinn, R. G., 2011.
817 Atmospheric histories and global emissions of the anthropogenic hydrofluorocarbons HFC-365mfc,
818 HFC-245fa, HFC-227ea, and HFC-236fa. *J. Geophys. Res.* 116, D08304.

819 Weiss, R.F. and Prinn, R.G., 2011. Quantifying greenhouse-gas emissions from atmospheric
820 measurements: a critical reality check for climate legislation. *Phil. Trans. R. Soc. A* (2011) 369,
821 1925–1942.

822 Yao, B., Vollmer, M. K., Zhou, L. X., Henne, S., Reimann, S., Li, P. C., Wenger, A., and Hill, M.,
823 2012. In-situ measurements of atmospheric hydrofluorocarbons (HFCs) and perfluorocarbons
824 (PFCs) at the Shangdianzi regional background station, China. *Atmos. Chem. Phys.* 12, 10181-
825 10193.

826 Yokouchi, Y., Taguchi, S., Saito, T., Tohjima, Y., Tanimoto, H., Mukai, H., 2006. High frequency
827 measurements of HFCs at a remote site in east Asia and their implications for Chinese emissions,
828 *Geophys. Res. Lett.* 33, L21814.

829 Xu, Y., Zaelke, D., Velders, G. J. M., and Ramanathan, V, 2013. The role of HFCs in mitigating
830 21st century climate change, *Atmos. Chem. Phys.* 13, 6083-6089.

831

832 **Supplementary Material**

833

834 **1. The observing network**

835 We used HFC atmospheric data from four European stations embedded in the global AGAGE
836 network and classified as WMO GAW (World Meteorological Organisation-Global Atmosphere
837 Watch) global. Two stations are mountain continental: Monte Cimone (CMN), located on the
838 highest peak of the Northern Apennines in Italy (at 2165 m above sea level) at the border between
839 continental Europe and the Mediterranean Basin and Jungfrauoch (JFJ), 3580 m above sea level,
840 located on a mountain saddle in the central Swiss Alps. Both stations are well suited for long-term
841 monitoring of trace gas concentration trends in the free troposphere. In addition, the proximity to
842 important anthropogenic source regions in central Europe, like e.g. the Po basin, makes them
843 appropriate for regional source allocation studies. Mace Head (MHD), located on the west coast of
844 Ireland, is exposed to the North Atlantic Ocean and is therefore the ideal location to study both
845 natural and man-made trace constituents in marine and continental air masses. Zeppelin (ZEP) is
846 located in the Arctic on Zeppelin Mountain, 474 meters a.s.l, close to the town of Ny-Ålesund
847 (Svalbard Islands, Norway), one of the world's northernmost human settlements. The site is well
848 suited for the monitoring of global atmospheric change and long-range pollution transport.

849

850 **2. Analytical methods**

851 Long term, high-frequency, high-precision measurements of HFCs are performed with gas
852 chromatographic-mass spectrometric (GC-MS) instruments equipped with pre-concentration
853 systems. At JFJ, MHD and ZEP the equipment currently used is an Agilent 5975 mass spectrometer
854 coupled to a Medusa pre-concentration system that allows cooling to $\sim -165^{\circ}\text{C}$ and trapping
855 compounds in a micro-trap filled with relatively mild adsorbent (Miller et al., 2008). 2 L samples of
856 ambient air are analysed every two hours, alternated with 2 L reference gas (working standard).
857 CMN uses the same MS instrument but with a different pre-concentration unit that allows trapping

858 compounds at -30°C in a multi-bed trap filled with adsorbents of increasing adsorption capacity
859 (Markes International, UNITY2-Air Server2); the higher trapping temperature limits the total
860 volume sampled to 1 L. Also in this case, ambient air samples analyses are alternated with 1 L
861 working standard analyses (Maione et al., 2013). In spite of the differences in the analytical
862 methodologies, measurements at the four stations are fully inter-comparable, because the same
863 calibration protocol is used: the working standards are air samples pumped at the stations during
864 relatively clean-background conditions into 35 L electro-polished stainless steel canisters (Essex
865 Cryogenics, Missouri) using a modified oil-free compressor (SA-3, RIX California) up to ~ 60 bar.
866 The tanks are humidified with purified water during the pumping process in order to improve the
867 stability of the compounds (Miller et al., 2008). The working standards are calibrated weekly
868 against a tertiary standard prepared at MHD and in turn calibrated against the SIO-2005 (Scripps
869 Institution for Oceanography) scale, where primary gravimetric standard are prepared.

870

871 **3. Inversion method**

872 3.1 Bayesian Inversion

873 In order to derive the emissions of nine HFCs from the European domain, high-frequency trace gas
874 atmospheric data have been combined with high-resolution atmospheric transport simulations. For
875 this aim we run the FLEXPART stochastic model that has a detailed treatment of turbulence and
876 convection (Stohl et al., 1998; 2005; Seibert and Frank, 2004) and employs meteorological analyses
877 from the European Centre for Medium-Range Weather Forecasts (ECMWF). We used the ECMWF
878 analyses at 1° of latitude \times 1° longitude resolution. FLEXPART was run backward in time from the
879 measurement stations at 3-hourly intervals, using 40000 particles for each backward run. The
880 particles were followed for 20 days with the aim of establishing the so-called source–receptor
881 relationship (SRR) between the potential HFC emission sources and the changes in mixing ratios
882 observed at each measurement station. Due to the HFC low reactivity, no loss process has been
883 considered. SRR (in units of s kg^{-1}) in a particular grid cell is proportional to the particle residence

884 time in that cell and measures the simulated mixing ratio at the receptor that a source of unit
885 strength (1 kg s^{-1}) in the cell would produce (Stohl et al., 2009). The SRR is also called “footprint”
886 or “emission sensitivity”.

887 Figure 1S shows the SRR obtained from two years of FLEXPART backward calculations using the
888 entire network of stations. There is not a homogenous sensitivity over the domain, this hinders the
889 ability of the inversion to determine emission source strengths over the entire domain with the same
890 accuracy. Therefore, there are areas, like e.g. the Scandinavia region and Eastern Europe, with a
891 lower sensitivity with respect to the rest of the domain.

892 For HFC-152a, the species with the shortest atmospheric lifetime (567 d), 3.5% in mass would be
893 lost after the maximum transport time of 20 d, which introduces a systematic under-prediction of
894 the emissions in the inversion not higher than 3.5%, whatever is the compound considered.

895 The contribution of each grid cell to the mixing ratios at the receptor is obtained by multiplying the
896 SRR values by the emission flux densities (in units of $\text{kg m}^{-2} \text{ s}^{-1}$) in that cell. The spatial
897 integration of each cell contributions gives the simulated mixing ratios at the receptor.

898 The inversion procedure used in this paper for estimating both emission strength and distribution
899 over the domain influencing the measurement sites is based on the analytical inversion method of
900 Seibert (2000, 2001), improved by Eckhardt et al. (2008). The inversion algorithm models the
901 emission field with the aim of optimizing the agreement between the measured and model
902 simulated concentration, considering at the same time *a priori* emissions and the uncertainties in
903 emissions, observations and model simulations.

904 Stohl et al. (2009) further improved the method considering a baseline in the observations that is
905 adjusted as part of the inversion process and adding a more detailed quantification of errors. All the
906 mathematical details of the method used in this study are described by Stohl et al. (2009).

907 The cost function J to be minimized is:

908

909
$$J = (M\tilde{x} - \tilde{y})^T \text{diag}(\sigma_0^{-2})(M\tilde{x} - \tilde{y}) + \tilde{x}^T \text{diag}(\sigma_x^{-2})\tilde{x} \quad (\text{Eq.1})$$

910 This function is composed of two terms: the first term on the right hand side measures the model-
911 observation misfit while the second term measures the deviation from the *a priori* values. In the
912 equation M represents the SRR matrix elements determined by model simulations; \tilde{x} is the
913 difference between the *a posteriori* and *a priori* emission vector and \tilde{y} is the difference between the
914 observed and the simulated *a priori* mixing ratio vector, respectively; σ_0 and σ_x are the error vector
915 in the observations and the vector of errors of the *a priori* values, respectively. The $\text{diag}(a)$ yields a
916 diagonal matrix with the elements of a in the diagonal.

917 The inversions have been performed with a variable resolution grid. The grid resolution was related
918 to the sensitivity: in the vicinity of the receptor a maximum resolution of $0.5^\circ \times 0.5^\circ$ was used
919 whereas further away the resolution becomes lower, down to $2^\circ \times 2^\circ$.

920

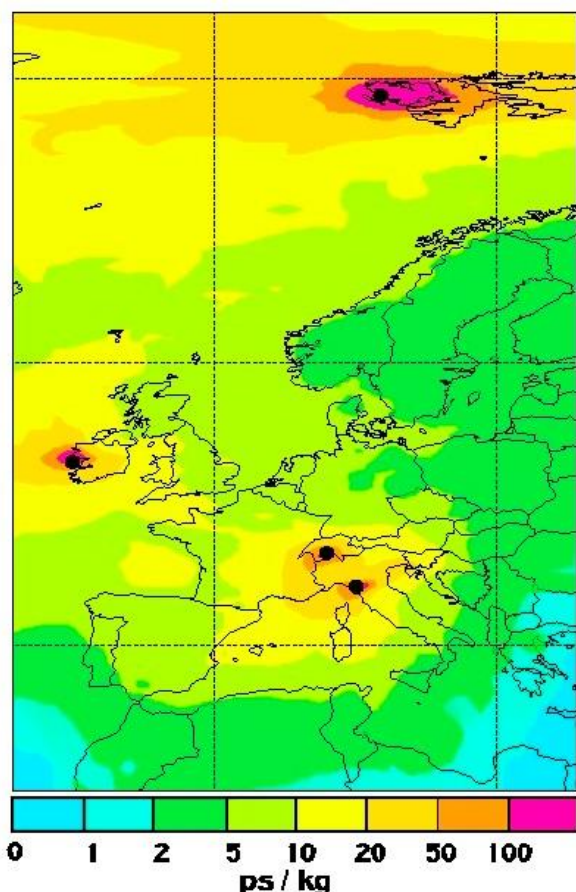
921

922

923

924

925



926

927 Figure 1S. Footprint emission sensitivity in picoseconds per kilogram (ps kg^{-1}) obtained from FLEXPART 20 d
 928 backward calculations averaged over all model calculations, over two years (Jan 2008- Dec 2009). Measurement sites
 929 are marked with black dots.

930

931 3.1.1 *A priori* emission field

932 For creating the most suitable *a priori* emission field to be adopted in the inversion, hereinafter
 933 called reference *a priori* field (RPF), we evaluated the best agreement between the observation data
 934 and the *a priori* simulated mixing ratios (modelled time series) produced using two different data
 935 bases. The simulated mixing ratios at each receptor point were obtained from the gridded *a priori*
 936 emissions multiplied by the gridded FLEXPART emission sensitivities. The reference emissions
 937 (REs) are those obtained using the RPF. We tested two different *a priori* emission fields. The first
 938 one is based on the annual national emissions as reported to the UNFCCC disaggregated within
 939 each country borders according to a gridded population density data set (CIESIN, Center for
 940 International Earth Science Information Network, www.ciesin.org). The second data base tested is
 941 the EDGARv4.2FT2010 (Emission Database for Global Atmospheric Research, version 4.2,

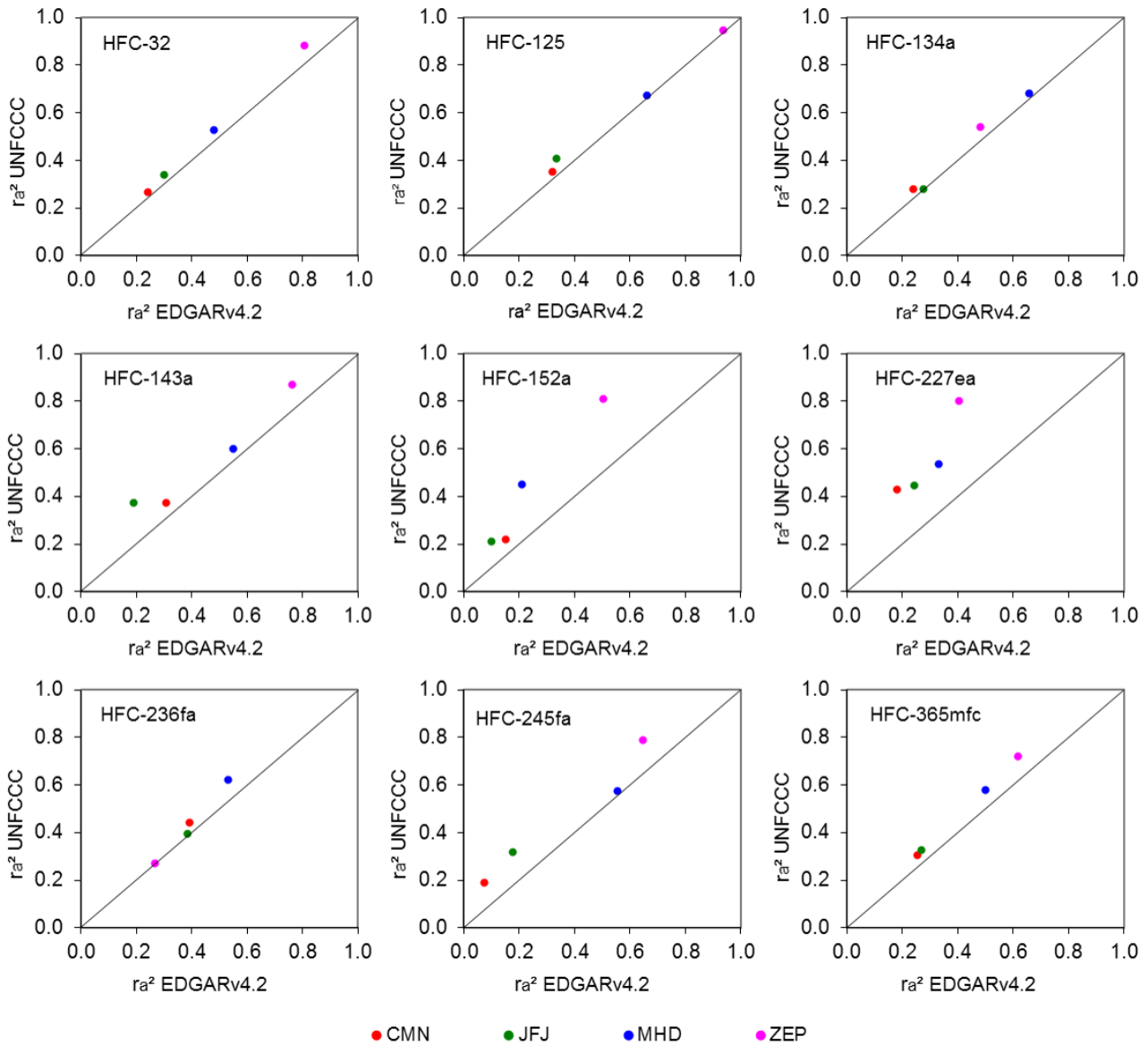
942 hereinafter EDGAR) inventory, which provides details on the emission distribution over the
943 domain, in a grid map with $0.1^\circ \times 0.1^\circ$ resolution. The most recent EDGAR data are for 2010 and a
944 linear extrapolation based on eleven-year emission trends (1998-2010) was used to extract the
945 emission values from 2011 to 2014.

946

947 In Figure 2S are reported the Pearson correlation coefficients r_a^2 between observations and the *a*
948 *priori* time series of both databases, obtained for each station and for each compound for 2012,
949 being the year in which the complete time series for all gases at all the four stations are available.

950 On the base of this criterion, UNFCCC emerged as the *a priori* emission field better correlated with
951 the observations of the HFCs considered. This is particularly evident for compounds like HFC-152a
952 and HFC-227ea, as shown in Figure 2S.

953



954

955 Figure 2S. r_a^2 Pearson correlation coefficients between the observations and the *a priori* time series of UNFCCC vs
 956 EDGARv4.2FT2010, obtained for each station and for each compound.
 957

958 As no information is available on the uncertainty of emissions (σ_x) for both databases, we have to
 959 specify this uncertainty for every grid cell. For this purpose we have used $\sigma_j = p \max(1.2 x_j, 1.0$
 960 $x_{surf})$, where p is the uncertainty emission scale factor, x_j is the *a priori* emission flux in the
 961 inversion box j and x_{surf} is the average emission flux over the domain. We chose $p = 2$ after testing
 962 several alternative values. $p = 2$ appears to be the most appropriate because for higher values of p
 963 the obtained emission maps showed increasing levels of noise whereas lower values forced the

964 results close to the *a priori* field. Details on the parameterisation used here are described in Graziosi
965 et al., 2015.

966 Another source of information is the *European Pollutant Release and Transfer Register (E-PRTR)*,
967 where European member states must report the HFCs aggregated emission values for each industry
968 together with the geographical coordinates. However, since the information contained in the E-
969 PRTR is not available for the single HFCs, we increased by two the σ_j in the grid cells where the
970 HFC industries are located.

971

972 3.2 Sensitivity tests

973 With the purpose of estimating the influence of different uncertainty factors on the inversion results
974 we ran several sensitivity tests for each gas, obtaining a set of *a posteriori* emission fluxes. We ran
975 the sensitivity tests for 2012. The reduction of sigma values $\sigma_{x_priori}^j$ for each inverted grid cell to
976 an uncertainty value $\sigma_{x_posteriori}^j$ is due to the minimisation of the cost function J (Eq.1). After the
977 inversion we obtained an average uncertainty $\sigma_{x_posteriori}^j \cong 35\%$ over the study domain. As the
978 reduction of uncertainty in each grid box is linked to the sensitivity of the grid itself, larger
979 reductions are obtained in regions well covered by the simulations, whereas low sensitivity regions
980 show a lower uncertainty reduction.

981 For characterising the test results we used the *Pd* parameter, defined as

982

$$983 \quad Pd = \frac{RE - Test}{RE} * 100$$

984

985 where *RE* is, as defined above, the reference emission and *Test* is the emission obtained in the
986 single tests described below.

987

988

989 3.3 A Priori field tests

990 3.3.1 *A priori* field modulation

991 With the aim of testing the influence of the *a priori* emission flux on the inversion results we
992 repeated the reference inversion, using three different *a priori* emission scaling factors: 0.5, 1 and 2.
993 We performed this test for each compound and the obtained *Pd* values are given in Fig. 3S. Results
994 obtained showed how the inversions, using the three different scaling factors of the *a priori*
995 emission field, are able to give rather constant *a posteriori* emission fluxes, with a *Pd* of 7%
996 (average of nine HFCs). When fewer receptors are available, the sensitivity of the domain
997 decreases, reducing the inversion capability to “correct” the *a priori* emission field. As a
998 consequence, when repeating the same analysis for a year in which the observations were available
999 for a lower number of receptors (2008, not shown), the average *Pd* value rose to 12%.

1000 The *Pd* value is inversely proportional to the sensitivity of the emitting area, highlighting that areas
1001 with higher sensitivity are more independent from the *a priori* field. On the whole, the average *Pd*
1002 values obtained suggest a good reliability of our emission estimates for all the gases considered in
1003 this study.

1004 3.3.2 Testing EDGAR as *a priori* emission field

1005 In order to assess to what extent the *a posteriori* emission fluxes obtained are affected by the *a*
1006 *priori* emission field used, we ran the inversions using as *a priori* emissions those given in the
1007 EDGAR database. In so doing, we test the capability of the inversion to converge to the same *a*
1008 *posteriori* flux starting from *a priori* emission fields different both in intensity and spatial
1009 distribution. In the plot in Figure 3S the *Pd* values obtained using the two different *a priori* fields
1010 are reported, showing that the difference between the REs obtained is always within the error bar
1011 associated with our estimates. The compounds exhibiting higher *Pd* values are HFC-32 and 1’HFC-
1012 227ea, which starting from a ratio in the *a priori* emissions ((UNFCCC-EDGAR)/UNFCCC*100)
1013 of 76% and -590% converge to a ratio of 29% and -30%, respectively). This test confirmed the

1014 robustness of the method, highlighting how the emission fluxes calculated through the inversion are
1015 not greatly affected by the database used to create the *a priori* emission field.

1016

1017 3.4 Numbers of stations included in the inversion

1018 With this test we investigated how sensitive the inversion results are to the number of stations used
1019 for the inversion itself. In order to do that, we compared the inversion results obtained with a full
1020 data set (data from four stations) with those obtained using three or two stations at a time.

1021

1022 3.4.1 Removing one station

1023 The *Pd* values are shown in Figure 3S. For all the nine HFCs considered the average of *Pd* values
1024 were 7%, 10%, 13% and 9% removing CMN (no_CMN), JFJ (no_JFJ), MHD (no_MHD) and ZEP
1025 (no_ZEP), respectively. These results suggest that the data sets from the different stations are quite
1026 consistent with each other in constraining the European total emissions, and show the robustness of
1027 the inversion method even when using a sub set of concentration data.

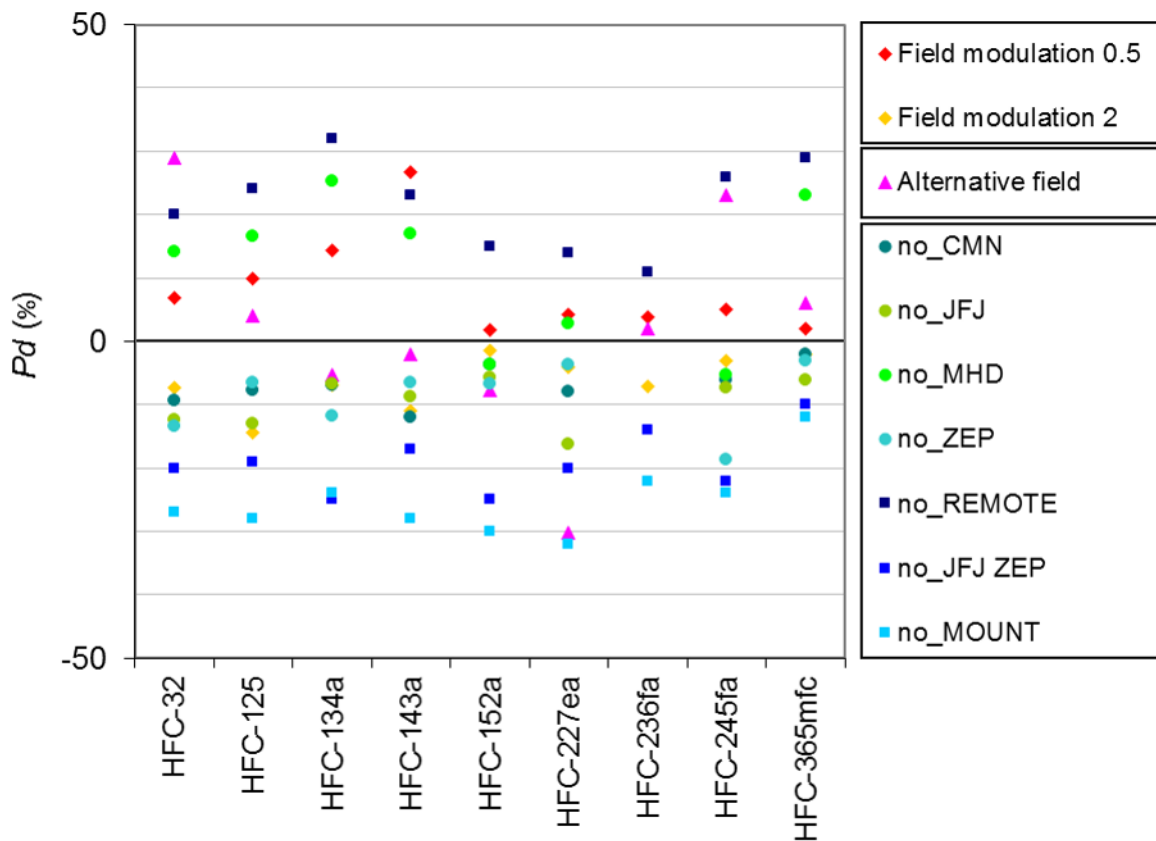
1028

1029 3.4.2 Removing station pairs

1030 The aim of this test was to evaluate to what extent the obtained emissions are affected by the
1031 removal of station pairs. We tested i) the removal of the mountain stations CMN and JFJ
1032 (no_MOUNT), both characterised by a complex topography, both affected by air mass trajectories
1033 not well reproduced and by close-by polluted regions; ii) the removal of MHD and ZEP
1034 (no_REMOTE), both scarcely affected by anthropogenic emissions; iii) the removal of JFJ and ZEP
1035 (no_JFJ ZEP), i.e. two stations with different characteristics.

1036 The obtained *Pd* values are summarized in Figure 3S, showing that the removal of two stations at a
1037 time produced a significant spread of the emissions values, with an *Pd* value over the EGD of 22%
1038 (average of nine HFCs), where the maximum variations are registered for HFC-134a (+32%
1039 NO_REMOTE) and HFC-227ea (-32% NO_MOUNT), respectively. It is noteworthy that the

1040 removal of the two mountain continental stations produced the highest variability, suggesting the
 1041 importance of including receptors affected by the strongest source areas. This test produced the
 1042 highest deviation from the inversion results.
 1043 Figure 3S shows the Pd values obtained from all the sensitivity tests and for all the compounds
 1044 considered.



1045
 1046
 1047 Figure 3S. Pd values obtained for nine HFCs through the sensitivity tests.

1048
 1049 3.5 Station model performance

1050 For assessing the inversion performance and evaluating the time series at the four stations, we show
 1051 HFC-134a statistical parameter values. Similar results, not shown, were obtained with the other
 1052 HFCs.

1053 The station-specific error statistics for 2012 were evaluated by comparing the *a posteriori* and *a*
1054 *priori* errors at the four stations, using several different statistical parameters. The relative error
1055 reduction $1 - E_b/E_a$ %, where E_a and E_b are the *a priori* and *a posteriori* Root Mean Square (RMS)
1056 errors was 14.2%, 20.1%, 33.1%, and 14.3% at CIMN, JFJ, MHD and ZEP, respectively (see also
1057 Table 1S). On the time scale of 20 days, also for a remote station like ZEP scarcely affected by
1058 source regions, the relative error reduction is similar as in the other sites. The two mountain
1059 stations, CMN and JFJ that are even closer to the source regions, show the highest observed values
1060 as well as the highest standard deviation (SD on table 1S). Nevertheless, we obtained lower, but still
1061 significant error reduction. The reason of this behaviour is due to the model problem linked to the
1062 complex topography of mountain stations. Generally, the model shows the best performance in
1063 areas with simple topography, where the meteorology is well described by the ECMWF data; this
1064 aspect is largely discussed in previous papers (Stohl et al., 2009, Maione et al., 2014 and Graziosi et
1065 al., 2015). As a consequence, for the two mountain stations r_a^2 and r_b^2 values lower than those at the
1066 others stations are observed.

1067 The squared Pearson correlation coefficient r_{ba}^2 (and r_{bb}^2) between the *a priori* (and *a posteriori*)
1068 baseline and the observed concentrations describes the baseline variability and trend. The *a priori*
1069 signal for CMN, JFJ, MHD, and ZEP are 22%, 11%, 40% and 60% respectively. The higher values
1070 obtained for the remote stations are due to the lower occurrence of pollution events.

1071 A comparison between the modelled time series and the observations at the receptors is used to
1072 evaluate the proximity of the modelled emission field to the actual one. The ability of the model to
1073 reproduce the values above the baseline is described by the correlation analysis of the polluted
1074 events with the simulated emission contributions, described by the *a priori* (r_{ea}^2) and the *a*
1075 *posteriori* (r_{eb}^2) values (Table 1S).

1076

1077

1078 Table 1S: Station parameters. Mean, mean HFC-134a mixing ratios; SD, standard deviation of the observed mixing
 1079 ratios; N, number of observations; E_a , RMS *a priori* error; E_b , RMS *a posteriori* error; $1-E_a/E_b$, relative error reduction;
 1080 r_a^2 and r_b^2 , squared Pearson correlation coefficients between the observations and the *a priori* (r_a^2) and *a posteriori* (r_b^2)
 1081 simulated time series; r_{ba}^2 (and r_{bb}^2) is the squared Pearson correlation coefficients between the *a priori* (and *a*
 1082 *posteriori*) baseline and the measured concentrations; r_{ea}^2 (and r_{eb}^2) is the squared Pearson correlation coefficients
 1083 between the *a priori* (and *a posteriori*) enhancements above the baseline and the measured concentrations.
 1084

Station	Mean (ppt)	SD (ppt)	N	E_a (ppt)	E_b (ppt)	1- E_b/E_a %	r_a^2	r_b^2	r_{ba}^2	r_{bb}^2	r_{ea}^2	r_{eb}^2
CMN	80.58	7.40	2030	6.7	5.8	14.2	0.28	0.39	0.22	0.26	0.16	0.22
JFJ	76.44	4.74	2112	4.4	3.5	20.1	0.28	0.46	0.11	0.17	0.20	0.36
MHD	74.82	3.98	2483	2.8	1.9	33.1	0.66	0.79	0.40	0.44	0.45	0.56
ZEP	73.73	2.63	1716	1.8	1.6	14.3	0.54	0.65	0.60	0.62	0.31	0.38

1085

1086

1087

1088 **European annual emissions**

1089 In the following tables (Tables 2Sa-i) we report for each compound annual emissions and the
 1090 associated percent error from the EGD and from the twelve macro-areas considered in this study.

1091 Table 2S: Annual estimated emissions (Mg y⁻¹) and associated percent uncertainty, from the European Geographic
 1092 Domain (EGD) and from twelve macro-areas in Europe for nine HFCs: a) HFC-32; b) HFC-125; c) HFC-134a; d) HFC-
 1093 143a; e) HFC-152a; f) HFC-227ea; g) HFC-236fa; h) HFC-245fa; i) HFC-365mfc.
 1094

1095 a)

HFC-32	<err %>	2003	2004	2005	2006	2007	2008	2009	2010	2011	2012	2013	2014	<>
EGD							2229	1920	2393	2330	2852	2370	2352	2350
AT	22%						57	6	13	19	50	11	38	28
BE-NE-LU	15%						13	104	74	146	166	84	80	95
CH	24%						5	13	4	24	13	7	8	11
DE	28%						150	118	99	77	229	170	165	144
ES-PT	45%						412	284	537	475	373	423	456	423
FR	32%						388	385	395	444	689	371	331	429
IE	18%						34	30	41	39	39	69	52	43
IT	26%						316	322	524	484	479	447	365	419
NEE	43%						330	172	112	166	267	240	241	218
SCA	83%						89	164	124	109	108	88	64	106
SEE	63%						219	42	170	163	213	141	127	153
UK	23%						217	282	299	184	226	319	426	279

1096

1097 b)

HFC-125	<err %>	2003	2004	2005	2006	2007	2008	2009	2010	2011	2012	2013	2014	<>
EGD		4950	4608	5590	5795	7192	7174	5948	8313	7666	9864	7937	7324	7746
AT	20%	31	74	326	23	107	201	46	33	54	147	73	193	107
BE-NE-LU	22%	295	153	46	149	468	100	164	330	590	466	267	323	320
CH	36%	53	67	57	83	46	16	30	16	86	34	33	32	35
DE	35%	353	670	324	403	558	754	310	514	614	867	752	629	634
ES-PT	39%	882	517	665	813	717	900	842	1855	1303	1406	1514	1262	1297
FR	30%	816	786	1134	1192	881	1285	1044	1462	1398	2133	1652	1080	1436
IE	16%	75	115	99	128	118	174	158	215	180	175	211	206	188
IT	32%	982	799	1189	801	2162	717	872	1351	1254	1567	1455	887	1158
NEE	40%	475	117	595	795	607	870	861	424	755	761	654	762	727
SCA	80%	182	297	413	295	293	328	367	374	156	346	276	409	322
SEE	60%	238	228	121	249	236	899	99	501	702	1106	240	386	562
UK	19%	567	785	621	866	999	931	1155	1238	574	855	810	1155	960

1098

1099

1100

1101

1102

1103 c)

HFC-134a	<err %>	2003	2004	2005	2006	2007	2008	2009	2010	2011	2012	2013	2014	<>
EGD		24376	19690	20745	19232	19972	20478	18222	20608	18623	21611	19405	18347	19614
AT	26%	128	338	1416	267	640	724	325	222	226	279	222	566	366
BE-NE-LU	16%	1388	1127	633	924	885	542	626	714	1541	1377	719	886	915
CH	29%	153	512	238	280	130	123	159	102	175	155	127	122	137
DE	34%	3756	4347	1509	2465	4005	3218	1831	2482	2533	3845	2540	2600	2721
ES-PT	38%	6851	707	2115	1768	1599	1952	1768	2843	2013	1546	1540	2652	2045
FR	23%	3358	2104	4875	3819	3007	4060	3348	4346	3676	5304	4635	2714	4012
IE	12%	173	260	206	244	238	302	426	358	328	406	330	471	374
IT	25%	3456	3342	3039	2483	3859	2406	2458	3496	2410	2503	4285	1640	2743
NEE	38%	1828	791	1344	2364	1016	1496	1481	820	898	1020	1034	1587	1191
SCA	80%	375	1327	980	896	721	801	1531	915	532	974	605	843	886
SEE	56%	456	1393	1901	686	509	1505	913	795	1707	1576	922	1055	1210
UK	23%	2454	3441	2489	3036	3364	3349	3356	3516	2584	2626	2445	3211	3013

1104

1105

1106 d)

HFC-143a	<err %>	2003	2004	2005	2006	2007	2008	2009	2010	2011	2012	2013	2014	<>
EGD					4698	5529	6287	5679	6084	5398	7075	6030	5725	6040
AT	20%				34	65	128	22	46	28	62	52	89	61
BE-NE-LU	27%				129	277	72	292	217	419	398	256	276	276
CH	31%				11	27	11	26	8	61	21	27	23	25
DE	30%				377	288	758	400	462	631	560	625	488	561
ES-PT	36%				365	954	803	803	1206	1016	779	1229	802	948
FR	21%				1534	1051	1180	1066	1219	1056	1922	1257	949	1235
IE	19%				127	121	165	158	196	162	141	166	173	166
IT	33%				372	475	538	553	802	869	985	858	856	780
NEE	40%				658	787	1008	750	388	262	631	662	733	633
SCA	82%				228	232	372	557	326	276	241	189	197	308
SEE	64%				147	302	528	75	352	204	661	157	444	346
UK	31%				717	950	724	977	862	415	674	552	696	700

1107

1108

1109

1110

1111

1112

1113

1114

1115 e)

HFC-152a	<err %>	2003	2004	2005	2006	2007	2008	2009	2010	2011	2012	2013	2014	<>
EGD		5873	4220	5257	3454	5406	4287	2963	4469	3684	4016	3115	2839	3625
AT	25%	143	129	297	16	126	139	25	219	29	57	118	74	94
BE-NE-LU	23%	208	189	128	115	187	121	149	105	228	254	97	110	152
CH	33%	81	24	92	16	16	10	20	13	41	28	19	7	20
DE	37%	1046	1076	425	381	643	336	238	356	444	550	367	469	394
ES-PT	36%	765	250	901	545	467	349	131	864	153	130	177	153	280
FR	33%	758	491	743	490	404	585	372	539	449	567	550	281	478
IE	19%	26	16	11	19	10	17	27	32	15	26	24	33	25
IT	32%	620	576	885	590	1553	947	660	978	866	636	597	479	738
NEE	55%	366	166	379	360	805	442	595	388	408	488	327	309	422
SCA	80%	390	476	611	456	608	504	141	423	152	348	296	400	323
SEE	69%	1243	587	576	310	353	635	376	373	696	712	345	333	496
UK	26%	227	239	210	157	234	201	228	179	202	220	197	191	203

1116

1117 f)

HFC-227ea	<err %>	2003	2004	2005	2006	2007	2008	2009	2010	2011	2012	2013	2014	<>
EGD							348	348	408	435	489	435	432	414
AT	41%						0,0	0,0	0,0	0,4	0,0	0,3	2,1	0,4
BE-NE-LU	40%						5	16	23	53	8	15	14	19
CH	48%						1,0	1,2	0,2	1,2	1,2	0,4	0,3	0,8
DE	52%						59	53	63	54	103	64	24	60
ES-PT	62%						40	41	53	69	21	67	54	49
FR	48%						66	85	82	62	155	92	81	89
IE	41%						5	6	6	5	7	10	8	7
IT	47%						40	40	40	38	48	39	38	40
NEE	64%						31	28	40	45	29	35	48	37
SCA	81%						10	16	10	28	16	5	25	16
SEE	74%						25	5	12	5	35	13	22	17
UK	45%						67	56	79	75	66	95	117	79

1118

1119

1120

1121

1122

1123

1124

1125

1126

1127 g)

HFC-236fa	<err %>	2003	2004	2005	2006	2007	2008	2009	2010	2011	2012	2013	2014	<>
EGD							24	19	17	24	22	26	25	22
AT	57%						0,0	0,0	0,1	0,0	0,0	0,0	0,0	0,0
BE-NE-LU	56%						0,2	0,2	0,2	0,1	0,1	0,1	0,0	0,1
CH	52%						0,0	0,0	0,0	0,1	0,0	0,0	0,0	0,0
DE	64%						2,9	3,9	2,4	5,1	4,6	3,2	3,7	3,7
ES-PT	80%						6,5	3,7	1,8	4,4	4,7	3,2	3,7	4,0
FR	59%						1,1	0,8	0,8	0,7	0,7	1,1	0,8	0,8
IE	52%						0,0	0,0	0,1	0,0	0,1	0,0	0,1	0,0
IT	60%						0,9	0,8	0,4	0,3	0,6	0,7	0,6	0,6
NEE	74%						7,7	6,6	6,7	8,0	9,5	3,8	15,0	8,2
SCA	98%						1,9	2,2	3,5	3,9	1,5	1,7	0,5	2,2
SEE	87%						1,8	0,1	0,3	0,8	0,2	11,2	0,0	2,0
UK	60%						0,6	1,2	0,7	0,5	0,4	0,4	0,9	0,7

1128

1129 h)

HFC-245fa	<err %>	2003	2004	2005	2006	2007	2008	2009	2010	2011	2012	2013	2014	<>
EGD							917	686	751	641	788	694	688	738
AT	35%						2	3	8	3	11	18	11	8
BE-NE-LU	35%						38	59	39	48	51	39	58	47
CH	34%						2	2	2	6	4	4	4	3
DE	40%						35	66	64	53	106	74	61	66
ES-PT	48%						216	112	214	103	44	46	80	116
FR	37%						81	98	88	93	176	150	121	115
IE	27%						19	11	10	10	15	8	12	12
IT	38%						184	131	143	143	159	168	131	151
NEE	45%						89	45	28	27	34	30	47	43
SCA	83%						70	61	42	23	19	45	40	43
SEE	71%						68	29	29	60	123	52	42	58
UK	41%						113	70	82	73	46	59	79	75

1130

1131

1132

1133

1134

1135

1136

1137

1138

1139

1140 i)

HFC-365mfc	<err %>	2003	2004	2005	2006	2007	2008	2009	2010	2011	2012	2013	2014	<>
EGD				1188	1340	1433	1135	941	1093	1114	1316	943	1067	1087
AT	45%			9	5	10	11	2	7	6	29	3	28	12
BE-NE-LU	45%			50	70	76	50	50	68	184	139	73	85	93
CH	47%			7	17	4	4	3	1	9	7	4	3	5
DE	51%			75	48	198	112	65	140	113	219	168	113	133
ES-PT	55%			220	203	311	315	233	191	222	135	103	99	185
FR	46%			276	321	195	213	216	227	221	364	245	231	245
IE	41%			36	80	37	26	14	18	15	19	18	25	19
IT	43%			95	196	254	147	96	176	131	136	142	108	134
NEE	52%			47	62	34	31	56	55	30	55	45	117	55
SCA	87%			56	48	34	64	37	35	47	56	25	52	45
SEE	64%			58	29	24	21	48	43	56	76	17	45	44
UK	44%			260	262	256	141	121	132	79	81	101	162	116

1141

1142

1143

1144

1145 References

1146

1147 Eckhardt, S., Prata, A. J., Seibert, P., Stebel, K., and Stohl, A., 2008. Estimation of the vertical
1148 profile of sulfur dioxide injection into the atmosphere by a volcanic eruption using satellite column
1149 measurements and inverse transport modelling. Atmos. Chem. Phys. 8, 3881–3897.

1150

1151 EDGAR (Emission Database for Global Atmospheric Research, release version 4.2FT2010.

1152 European Commission, Joint Research Centre (JRC)/Netherlands Environmental Assessment
1153 Agency (PBL), 2011. <http://edgar.jrc.ec.europa.eu/EDGAR>

1154

1155 Graziosi, F., Arduini, J., Furlani, F., Giostra, U., Kuijpers, L. J. M., Montzka, S. A., Miller, B. R.,

1156 O'Doherty, S. J., Stohl, A., Bonasoni, P., and Maione, M., 2015. European emissions of HCFC-22

1157 based on eleven years of high frequency atmospheric measurements and a Bayesian inversion

1158 method. Atmos. Environ. 112, 196-207.

1159

1160 Maione, M., Giostra, U., Arduini, J., Furlani, F., Graziosi, F., Lo Vullo, E. Bonasoni, P., 2013.
1161 Ten years of continuous observations of stratospheric ozone depleting gases at Monte Cimone
1162 (Italy) - Comments on the effectiveness of the Montreal Protocol from a regional perspective. *Sci.*
1163 *Tot. Environ.* 445–446, 155–164.

1164

1165 Miller, B.R., Weiss, R.F., Salameh, P.K., Tanhua, T., Grealley, B.R., Mühle, J., Simmonds, P.G.,
1166 2008. Medusa: A sample pre-concentration and GC/MS detector system for in situ measurements
1167 of atmospheric trace halocarbons, hydrocarbons, and sulphur compounds. *Anal. Chem.*, 80, 1536-
1168 1545.

1169

1170 Seibert, P., 2000. Inverse modelling of sulphur emissions in Europe based on trajectories, in:
1171 *Inverse Methods in Global Biogeochemical Cycles*, edited by: Kasibhatla P., Heimann M., Rayner
1172 P., Mahowald N., Prinn R. G., and Hartley D. E., 147–154, *Geophysical Monograph 114*, American
1173 Geophysical Union, ISBN:0-87590-097-6.

1174

1175 Seibert, P., 2001. Inverse modelling with a Lagrangian particle dispersion model: application to
1176 point releases over limited time intervals, In: *Air Pollution Modeling and its Application XIV*,
1177 edited by: Schiermeier F. A. and Gryning S.-E., Kluwer Academic Publ., 381–389.

1178

1179 Seibert, P., and Frank, A., 2004. Source-receptor matrix calculation with a Lagrangian particle
1180 dispersion model in backward mode. *Atmos. Chem. Phys.* 4, 51–63.

1181

1182 Stohl, A., Hittenberger M., and Wotawa G., 1998. Validation of the Lagrangian particle dispersion
1183 model FLEXPART against large scale tracer experiment data. *Atmos. Environ.* 32, 4245–4264.

1184

1185 Stohl, A., Forster, C., Frank, A., Seibert, P., Wotawa, G., 2005. Technical note: The Lagrangian
1186 particle dispersion model FLEXPART version 6.2. *Atmos. Chem. Phys.* 5, 2461–2474.

1187

1188 Stohl, A., Seibert, P., Arduini, J., Eckhardt, S., Fraser, P., Grealley, B. R., Lunder, C., Maione, M.,
1189 Mühle, J., O'Doherty, S., Prinn, R. G., Reimann, S., Saito, T., Schmidbauer, N., Simmonds, P. G.,
1190 Vollmer, M. K., Weiss, R. F., and Yokouchi, Y., 2009. An analytical inversion method for
1191 determining regional and global emissions of greenhouse gases: Sensitivity studies and application
1192 to halocarbons. *Atmos. Chem. Phys.* 9, 1597-1620.

1193

1194

1195

1196

1197

1198